

UNITED STATES  
COMMITTEE ON LARGE DAMS

HYDRAULICS BRANCH  
OFFICIAL FILE COPY

PAP 457



Bureau of Reclamation  
HYDRAULICS BRANCH  
OFFICE  
FILE COPY  
WHEN BORROWED RETURN PROMPTLY

# Dam Safety and Rehabilitation

## Fourth Annual USCOLD Lecture

PAP 457

January 24, 1984

### USCOLD LECTURES

1981	James Bay Hydro Development
1982	Tarbella Dam Project, Pakistan
1983	Bath County Hydroelectric Pumped-Storage Project
1984	Dam Safety and Rehabilitation

### 1984 SPEAKERS

David L. Hinchliff –	Hydraulic Design and Application of Labyrinth Spillways
Edward W. Gray, Jr. –	Fuse Plug Embankments in Auxiliary Spillways Developing Design Guidelines and Parameters
Lloyd O. Timblin, Jr. –	Flexible Membrane Emergency Spillway
C. O. Duster –	Dam Crest Raising With Reinforced Earth Retaining Walls
L.R. Carpenter –	Automatic Monitoring of Structural Behavior Instruments for Reclamation Concrete Dams
Raymond G. Acciardi –	Improvements to USBR Pinhole Test Equipment - Design and Test Result Evaluation
Douglas Craft –	Chemical Tests for Dispersive Soils - Problems and Recent Research
Luther Davidson –	Electronic Monitoring of Cement Pressure Grouting at Ridgway Dam

## ERRATA

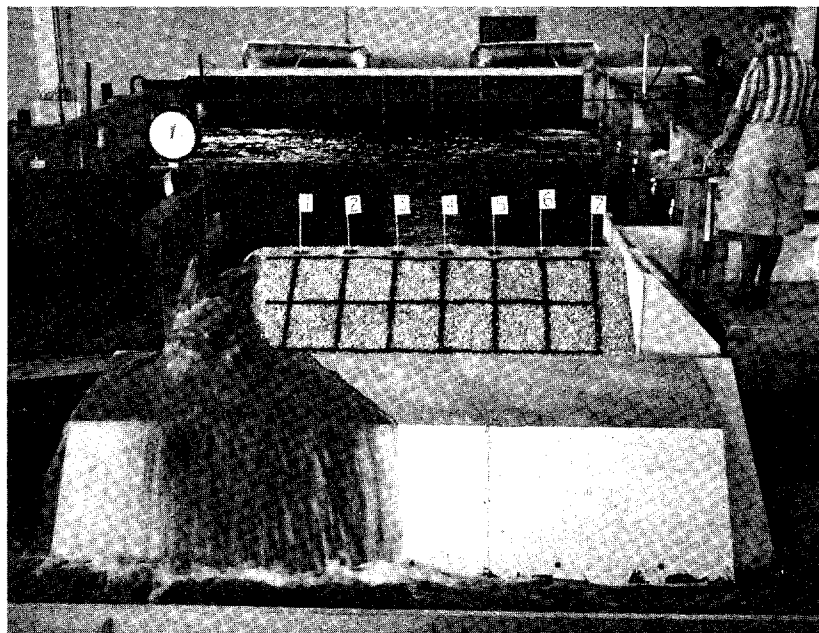
### Fourth Annual USCOLD Lecture

#### Fuse Plug Embankments in Auxiliary Spillways Developing Design Guidelines and Parameters

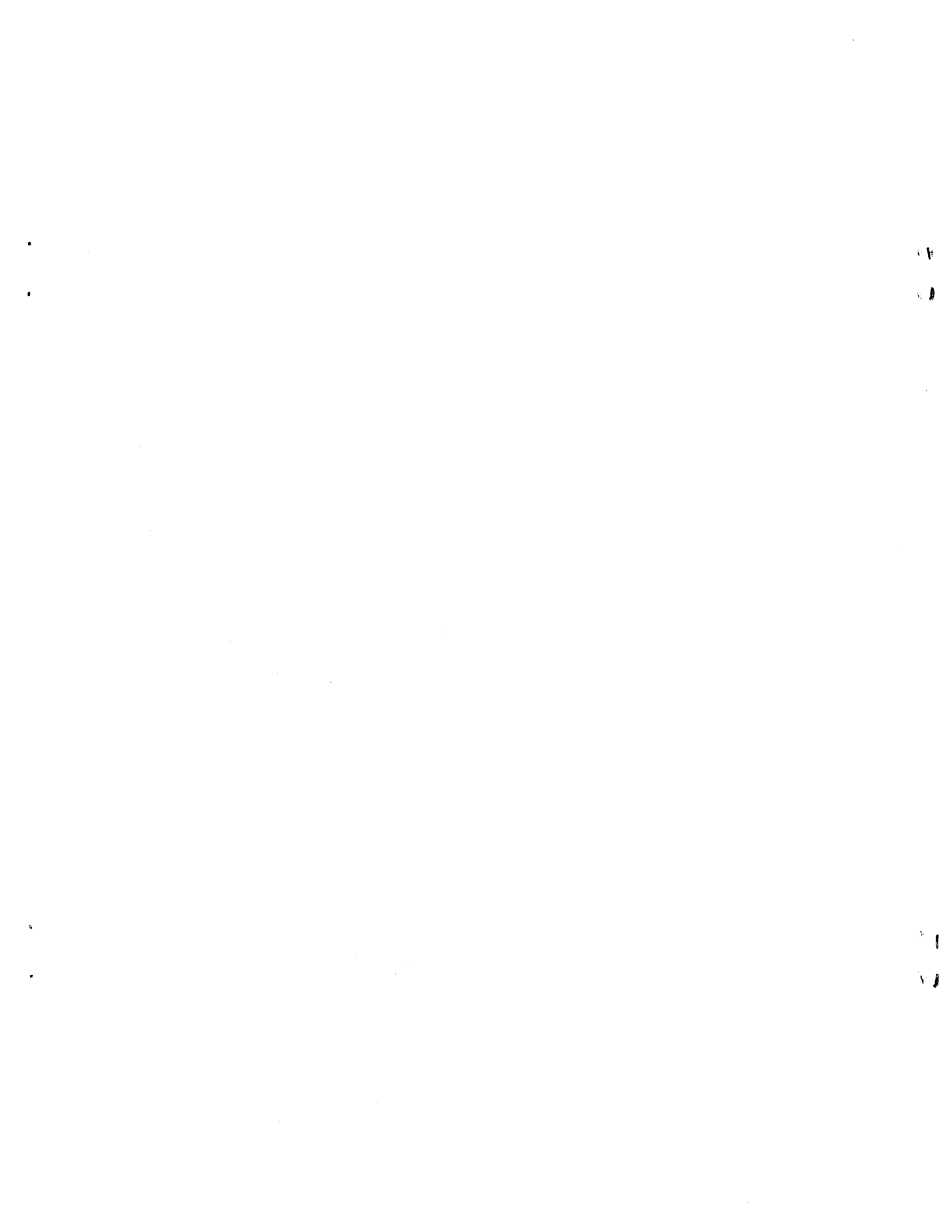
Page 2-v: The symbol for boundary or grain Reynolds number should read "R\*."

Page 2-20: Equation (9) should read " $\left(\frac{yL}{E}\right)_m = \left(\frac{yL}{E}\right)_p$ ."

Page 2-27: Figure 2-26(b) is not the correct photograph. The correct photograph is shown below.



Page 2-36: The eighth column heading in table 2-2 should read "p/H."



FUSE PLUG EMBANKMENTS  
IN AUXILIARY SPILLWAYS  
DEVELOPING DESIGN GUIDELINES  
AND PARAMETERS

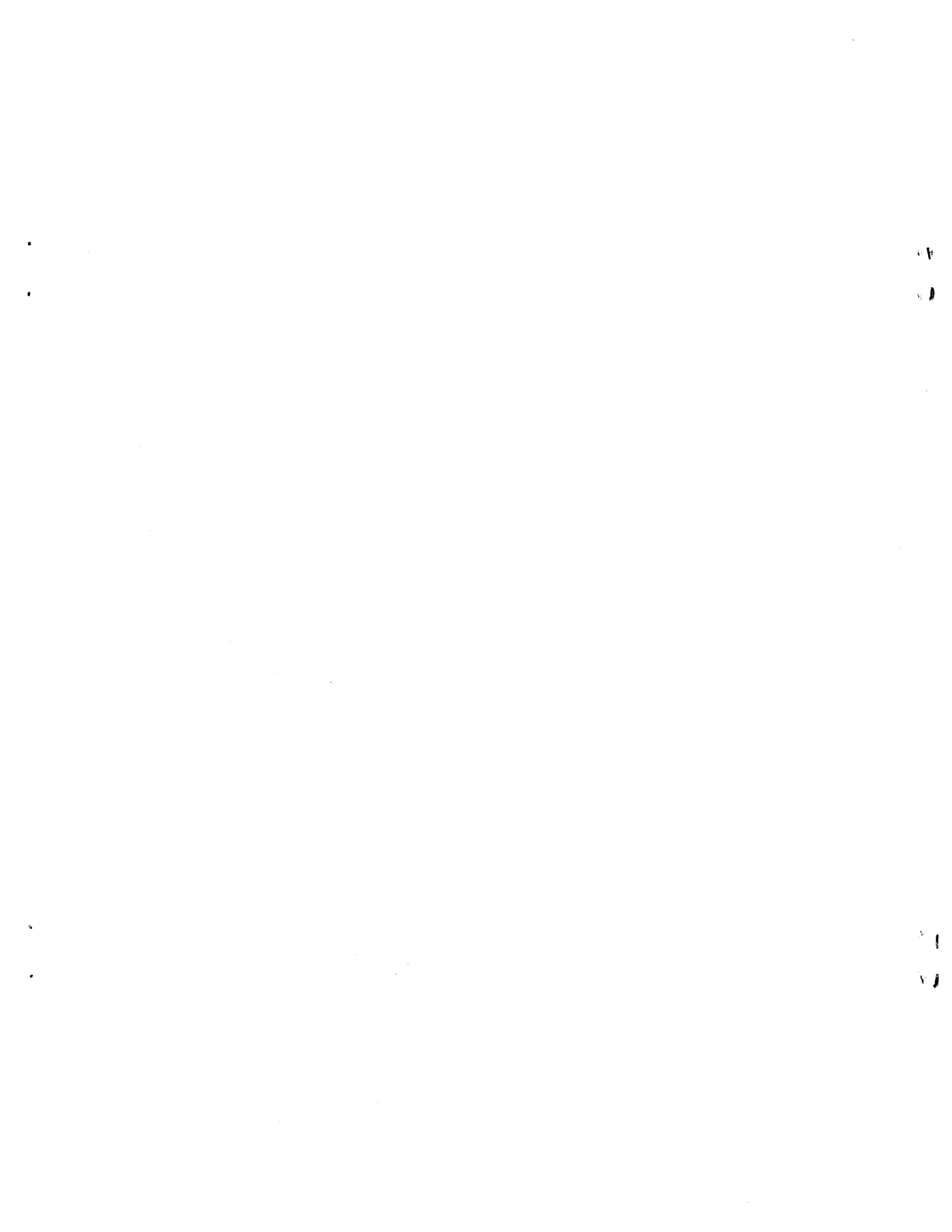
by

Clifford A. Pugh  
and  
Edward W. Gray, Jr.

January 1984

Hydraulics Branch - Division of Research and Laboratory Services  
Embankment Dams Branch - Division of Dam and Waterway Design  
Engineering and Research Center  
Bureau of Reclamation

Denver, Colorado



## CONTENTS

	Page
List of symbols . . . . .	2-v
Abstract . . . . .	2-vii
Introduction . . . . .	2-1
Conclusions . . . . .	2-1
Design guidelines . . . . .	2-2
Literature on fuse plug erosion . . . . .	2-3
The model . . . . .	2-4
Description . . . . .	2-4
Similitude . . . . .	2-7
Hydraulic similitude . . . . .	2-8
Dimensional analysis . . . . .	2-8
Sediment transport . . . . .	2-8
Settling velocity adjustment . . . . .	2-11
Erosion rate scale ratio . . . . .	2-11
Embankment design . . . . .	2-13
Structural similitude . . . . .	2-18
Model measurements . . . . .	2-20
Model results . . . . .	2-21
Analysis . . . . .	2-21
Effect of embankment design features . . . . .	2-21
Core . . . . .	2-21
Pilot channel . . . . .	2-30
Sand filter . . . . .	2-30
Size of embankment . . . . .	2-30
Hydraulics of flow through the opening . . . . .	2-31
Broad-crested weir . . . . .	2-31
Discharge coefficients . . . . .	2-31
Projection to prototype . . . . .	2-33
Comparison to Oxbow field test . . . . .	2-36
Bibliography . . . . .	2-37

## TABLES

Table		Page
2-1 Fuse plug model test data . . . . .		2-22
2-2 Oxbow field test data . . . . .		2-36

CONTENTS - Continued

FIGURES

Figure	Page
2-1 Model fuse plug embankment, test No. 7 . . . . .	2-5
2-2 Model operation, test No. 4 . . . . .	2-5
2-3 Flow measurement weir calibration curve . . . . .	2-6
2-4 Initial breach viewed through end wall, test No. 8 . . . . .	2-6
2-5 Forces on a sediment particle . . . . .	2-10
2-6 Dimensionless unit sediment discharge curves versus dimensionless shear and boundary Reynold's number . . . . .	2-10
2-7 Settling velocity of sand and silt in water ( $\frac{\rho_s}{\rho} = 2.65$ ) . . . . .	2-12
2-8 Fuse plug embankment and pilot channel . . . . .	2-14
2-9 Prototype gradation curves . . . . .	2-15
2-10 Gradation curves, sand filter . . . . .	2-15
2-11 Gradation curves, sand and gravel . . . . .	2-16
2-12 Gradation curves, slope protection . . . . .	2-16
2-13 Gradation curves, rockfill . . . . .	2-17
2-14 Model placement . . . . .	2-17
2-15 Fuse plug embankment after placement . . . . .	2-19
2-16 Flow through the pilot channel showing the failure mode of the impervious core . . . . .	2-19
2-17 Definition sketch of geometric features of model fuse plug embankment . . . . .	2-22
2-18 Lateral erosion rate, test No. 1 . . . . .	2-23
2-19 Lateral erosion rate, test No. 2 . . . . .	2-23
2-20 Lateral erosion rate, test No. 3 . . . . .	2-24
2-21 Lateral erosion rate, test No. 4 . . . . .	2-24
2-22 Lateral erosion rate, test No. 4 . . . . .	2-25
2-23 Lateral erosion rate, test No. 6 . . . . .	2-25
2-24 Lateral erosion rate, test No. 7 . . . . .	2-26
2-25 Lateral erosion rate, test No. 8 . . . . .	2-26
2-26 Photographs illustrating the washout process (3 sheets) . . . . .	2-27
2-27 Schematic of lateral erosion process . . . . .	2-32
2-28 Broad-crested weir flow profiles, test Nos. 6, 7, and 8 . . . . .	2-32
2-29 Weir formula discharge coefficients, test No. 7 . . . . .	2-34
2-30 Lateral erosion rate as a function of water depth and crest length . . . . .	2-34
2-31 Lateral erosion rates predicted from model tests . . . . .	2-35
2-32 Embankment design for Oxbow field test . . . . .	2-35

## LIST OF SYMBOLS

A	- Cross sectional area
B	- Width of base of fuse plug
b	- Width of base of fuse plug downstream from the core
C	- Discharge coefficient
C <sub>c</sub>	- Correlation coefficient
D	- Reservoir water depth above fuse plug base
d	- Sand grain diameter
d <sub>50</sub>	- 50 percent sand grain diameter
d <sub>90</sub>	- 90 percent sand grain diameter
E	- Modulus of elasticity
E <sub>l</sub>	- Lateral erosion rate
F	- Function of
f	- Friction factor
F	- Froude number
F <sub>c</sub>	- Critical tractive force
F <sub>w</sub>	- Weight force
g	- Gravitational acceleration
H	- Height of fuse plug
h	- Pilot channel depth
J	- Weir length
k <sub>s</sub>	- Equivalent sand grain roughness
L	- Distance along fuse plug crest
l	- Length
M	- Structural merit number
p	- Top length of pilot channel along crest
P	- Pressure
Q	- Water discharge
Q <sub>s</sub>	- Sediment discharge
q	- Unit discharge
q <sub>s</sub>	- Unit sediment discharge
q <sub>s</sub> <sup>*</sup>	- Dimensionless unit sediment discharge
R	- Hydraulic radius
R	- Reynolds number
R <sup>*</sup>	- Boundary or grain Reynolds number
S	- Water surface slope
S <sub>s</sub>	- Sand specific gravity
T	- Impermeable core thickness
t	- Clay core thickness in the model
t'	- Time
u <sup>*</sup>	- Shear velocity
V	- Average water velocity
w	- Sediment settling velocity
W	- Width of fuse plug crest in direction of flow
y	- Specific force of water
Y <sub>s</sub>	- Specific force of sediment
θ	- Angle of core with horizontal
ν	- Kinematic viscosity of fluid
ρ	- Density of fluid

LIST OF SYMBOLS - Continued

- $\rho_s$  - Density of sediment grain
- $\sigma$  - Surface tension
- $\sigma_g$  - Standard deviation of particle sizes
- $\tau_c$  - Critical shear stress
- $\tau_0$  - Bed shear stress
- $\tau^*$  - Dimensionless shear stress
- $\theta$  - Friction angle

---

Subscript  $r$  refers to the ratio between prototype and model values  
Subscript  $m$  refers to the model  
Subscript  $p$  refers to the prototype

## ABSTRACT

The increasing size of design floods is causing dam designers to investigate more cost-effective methods of providing additional spillway capacity. In many cases, auxiliary spillways with fuse plug embankments can provide an economical alternative to passing all the flow through concrete structures.

The Bureau of Reclamation undertook research to help develop design guidelines to be used in cases where a fuse plug embankment would be appropriate. The lateral rates of erosion and discharge coefficients determined during this research can be used to calculate the downstream flow with a computer flood-routing study.

Fuse plug embankment models were used during the research to study the erosion process. The models were designed according to the Froude law with adjustments made to compensate for low Reynolds numbers affecting the sediment transport rate.



## INTRODUCTION

Dam safety concerns have renewed interest in the use of fuse plugs as an economical alternative to installing gates in auxiliary spillways. A fuse plug is an embankment designed to wash out in a predictable and controlled manner when flow capacity in excess of the normal capacity of the service spillway and/or outlet works is needed. An uncontrolled overflow spillway with a high crest elevation would serve the same purpose; however, the uncontrolled spillway would have to be very wide to pass a large flow. A fuse plug controlled auxiliary spillway has the advantage of developing deeper flow after the embankment is washed away, thus allowing the spillway channel to be narrower. The increasing size of design floods for both existing and new dams is a major problem facing dam designers. Several methods are now available to provide spillway capacity for infrequently occurring floods. One of the most common and least expensive alternatives is to provide flood surcharge. Additional surcharge space, however, may not be available for several reasons: development along the reservoir shoreline, raising the dam crest may be impracticable, or additional reservoir head could result in damaging flows to existing waterway structures. Another alternative is to provide an auxiliary spillway. Constructing a fuse plug across the auxiliary spillway would restrict the operation of that waterway to floods of infrequent occurrence, much the same as the installation of gates. In many cases, auxiliary spillways with fuse plug embankments can provide an economical alternative to passing all of the flow through concrete structures. The fuse plug embankment is designed to preclude use of the auxiliary spillway during minor floods.

The auxiliary spillway may be located on an abutment of the dam or at some location on the reservoir rim, provided the discharge can be safely directed into an existing water course. The additional discharge capacity provided by an auxiliary spillway may be required for existing reservoirs when hydro-meteorological data acquired since construction have resulted in a revised IDF (inflow design flood) that is too large for the available surcharge space and the existing waterway structures to control safely. In the case of new construction, an auxiliary spillway, in combination with conventional structures, may provide a favorable, economical alternative for making required reservoir releases.

## CONCLUSIONS

- A properly designed fuse plug embankment will wash out in an orderly and predictable manner when additional flow capacity is needed to pass a large flood through a reservoir. The embankment will preclude use of the auxiliary spillway during small floods.
- The rate of washout (lateral erosion rate) is a function of the erosion rate of the embankment material and not a function of the impermeable core strength.
- The erosion rates and discharge coefficients determined in this study can be used in flood-routing computer programs to help design fuse plug embankments.

- The sand filter, embankment material, and gradation have significant effects on erosion rates.
- A model design method is described that compensates for the fact that the Reynolds number is normally too low to properly simulate sediment transport in a Froude scale hydraulic model. This method uses settling velocity adjustments and dimensionless unit sediment discharges to adjust the model grain sizes and/or the model sediment density.

## DESIGN GUIDELINES

A fuse plug is a zoned earth and rockfill embankment designed to wash out in a predictable manner when breached. The embankment materials are selected and placed so that a constant rate of lateral erosion will occur as the structure is breached.

The fuse plug is designed as a dam, stable for all conditions of a reservoir operation except for a flood that will cause it to breach. The washout of a fuse plug should begin at a preselected location; a washout caused by general overtopping of the entire fuse plug should not occur.

The preferred method is to initiate breaching of the fuse plug with reservoir water. When the reservoir level reaches a predetermined elevation, a low spot in the embankment crest, called a pilot channel, will be overtopped. By placing highly erodible materials in the pilot channel section, breaching will occur rapidly, and the remainder of the fuse plug embankment will wash out laterally at a constant, predictable rate without overtopping. The auxiliary spillway flow will increase at a constant rate. This automatic breach feature is desirable because it reduces the possibility of mechanical or human error at a time when operation of a flood relief mechanism is critical. When a wide auxiliary spillway is required, it may be desirable to sectionalize the fuse plug with concrete separation walls. By using successively higher elevations for the fuse plug crests and pilot channels in each section, the washout process can be matched with successively less frequently occurring floods. The entire fuse plug would not wash out unless the entire capacity of the auxiliary spillway was needed.

The rate of lateral erosion as the fuse plug washes out is of primary importance. The rate of increase in downstream flow is not only dependent upon the rate of lateral erosion, but also upon the elevation of the reservoir. The rate of lateral erosion depends on the gradations and types of materials used to construct the fuse plug, the depth of flow above the base of the fuse plug, and the geometry of the fuse plug section (crest width, angle of the outer slopes, and configuration of the zoning).

The total discharge through an auxiliary spillway with a fuse plug embankment is controlled by the elevation of the grade sill or nonerodible foundation beneath the fuse plug, the width of the spillway channel, and the depth of water above the grade sill or foundation. The maximum depth of water above the base of the fuse plug can be controlled by choosing a pilot channel elevation, which will be breached at a selected time during the IDF. It may be desirable, for instance, to breach the fuse plug early during a flood with

a high peak. This timing would provide double use of some of the surcharge storage space by evacuating that space early in the flood.

As a general rule, fuse plugs should be designed to operate only for floods with recurrence intervals that are long relative to the economic life of the project. Fuse plugs should not be designed to operate for floods with recurrence intervals less than 100 years.

The rates of lateral erosion and coefficients of discharge obtained from curves resulting from Bureau of Reclamation research can be used in a computer flood-routing program to predict the downstream flows and maximum reservoir water surface elevation. The effects of varying the rate of lateral erosion and the elevation of the pilot channel on the reservoir elevation and auxiliary spillway discharge can be determined.

The auxiliary spillway should be designed according to standard practice. The flow velocities must be sufficient for the water to carry the eroded fuse plug material downstream to avoid clogging of the return channel to the natural stream course. If excessive sediment deposition is anticipated, a site-specific model study may be required to design the return channel.

#### LITERATURE ON FUSE PLUG EROSION

In the past, fuse plug embankments have been designed and constructed for mine tailing dams, on levees, and to control flow in auxiliary spillways. However, there has not been a documented case of a fuse plug controlled spillway actually operating. Most of the information in the literature is associated with studies conducted in 1959 to design a fuse plug controlled spillway for the Oxbow Project, on the Snake River between Idaho and Oregon [1, 2, 3]\*.

The Oxbow Project has two spillways, each with a design flow capacity of 4,250 m<sup>3</sup>/s (150,000 ft<sup>3</sup>/s), which is on the order of the 100-year flood. The total discharge capacity of 8,500 m<sup>3</sup>/s (300,000 ft<sup>3</sup>/s) corresponds to the inflow design flood. The original design required three radial gates to control each spillway. Later, the Idaho spillway, on the right abutment, was changed to fuse plug control [3]. The studies conducted to confirm the design assumptions included 1:20 and 1:40 scale model tests in the laboratory and a 1:2 scale field test at the damsite.

Another study of erosion mechanics and washout time rates of erodible control embankments was made using hydraulic models at the University of Windsor, in 1977 [4]. This study analyzed theoretical equations and compared calculations with model results.

---

\* Numbers in brackets refer to entries in the Bibliography.

## THE MODEL

### Description

The model was designed to simulate typical prototype fuse plugs from 3 to 9 m (10 to 30 ft) high. The model embankments were from 0.15 to 0.38 m (0.5 to 1.25 ft) high and 2.7 m (8.8 ft) long at scales of 1:25 and 1:10, respectively (fig. 2-1). The model size was based on the maximum flow available in the laboratory. A flow of  $0.61 \text{ m}^3/\text{s}$  ( $21.5 \text{ ft}^3/\text{s}$ ) was made possible by using two pumps operated in parallel.

The overall model was 14 m (46 ft) long by 8 m (26 ft) wide. Flow entered the model through two 0.3-m (1-ft) pipes and passed through a rock baffle into a 7.6-m (25-ft) by 5.2-m (17-ft) by 1.5-m (5-ft) deep headbox (fig. 2-2). The headbox simulated a reservoir in a prototype structure. The water surface level in the headbox was controlled by a 7.6-m (25-ft) long adjustable-height weir along one side. Water flowing over the adjustable weir plunged into a side channel and then passed through a flow measurement weir. The flow measurement weir was calibrated for flow versus water surface elevation in the side channel. The measurement weir was a combination type. The lower 0.31 m (1 ft) of weir was a  $90^\circ$  V-notch. Above the V-notch were 0.61-m (2-ft) extensions on each side at a  $15^\circ$  angle with horizontal. Above these  $15^\circ$  extensions were 0.46-m (1.5-ft) long vertical sides. The calibration curve for the measurement weir is shown on figure 2-3. The calibration was done in three parts corresponding to the three different sections of the weir. During each test, the calibration curve shown on figure 2-3 was used to compute the discharge through the measurement weir.

The fuse plug embankment platform was located at the end of the headbox. The platform was placed at an elevation 0.76 m (2.5 ft) above the headbox floor. One end wall of the platform was constructed from transparent plastic to observe the initial breach and lateral erosion process (fig. 2-4). A sloping platform, downstream from the horizontal fuse plug platform, led to a tailbox where the sediment was deposited before the water returned to the laboratory supply reservoir. A typical test used the following procedure:

1. With the adjustable control weir at a low level, the valves controlling the two inlet pipes were opened; the entire flow of  $0.61 \text{ m}^3/\text{s}$  ( $21.5 \text{ ft}^3/\text{s}$ ) entered the headbox, passed over the control weir and through the measurement weir.
2. The test was started by raising the reservoir water surface (with the control weir) to a predetermined level where water began flowing through the pilot channel.
3. As the fuse plug embankment washed away, more water passed through the breach. The water surface was kept at a constant level by gradually raising the control weir.
4. The flow through the measurement weir, the level of the water surface in the reservoir, and the time were recorded continuously. Each test was videotaped; still photographs and slides were also taken.

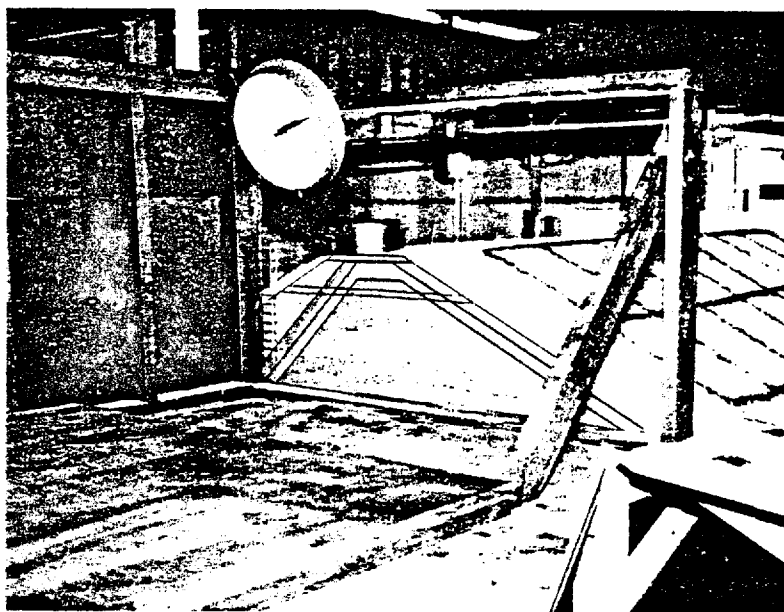


Figure 2-1. - Model fuse plug embankment, test No. 7.

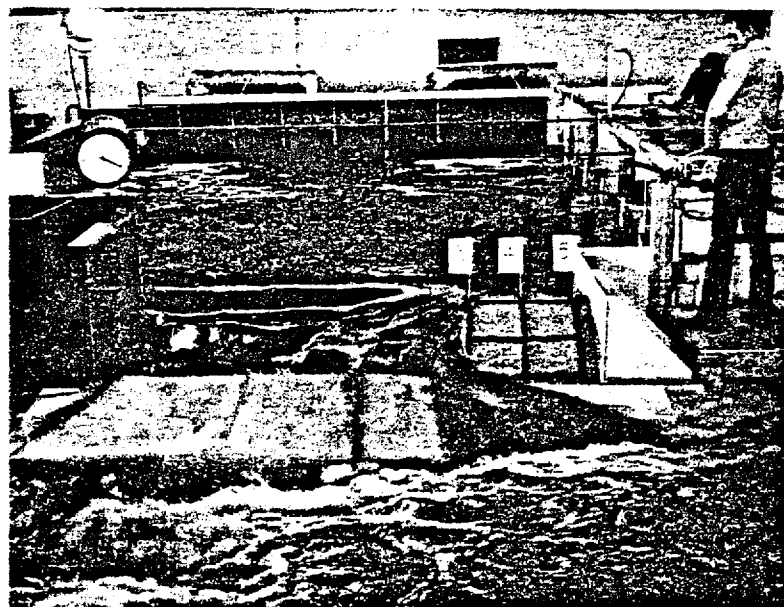


Figure 2-2. - Model operation, test No. 4. Water enters the model through the two pipes in the background. The water surface level is controlled by the long weir along the side.

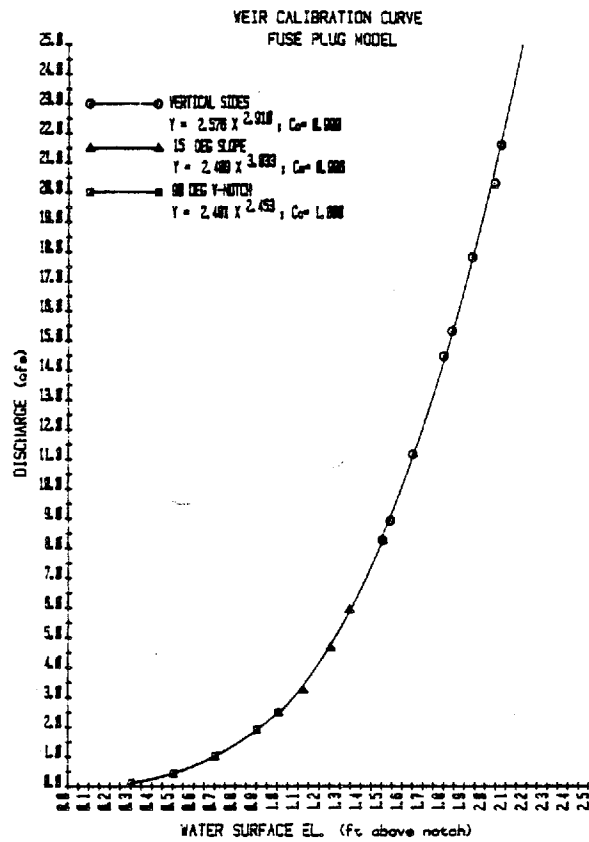


Figure 2-3. - Flow measurement weir calibration curve.

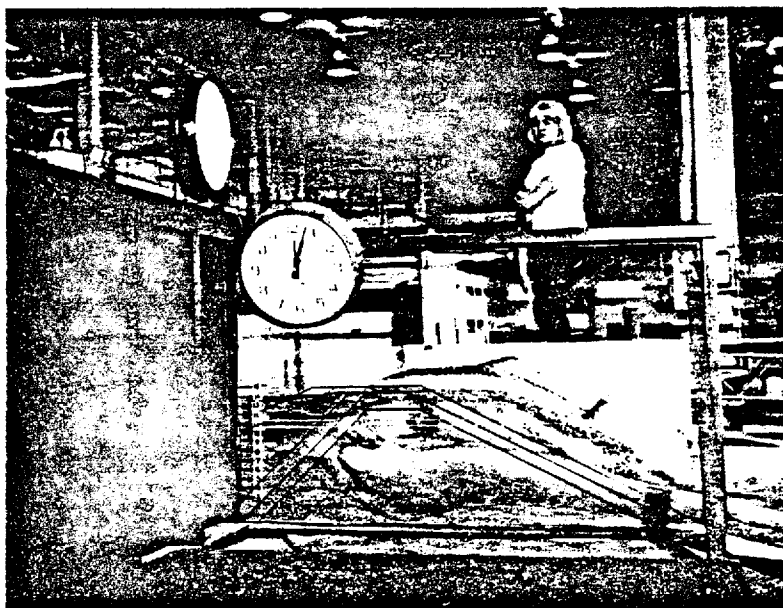


Figure 2-4. - Initial breach viewed through end wall, test No. 8.

5. Flows through the breach were computed by subtracting the measurement weir readings from the total (initial) flow.

### Similitude

Hydraulic model studies were used because of the large number of variables involved in hydraulic flow problems, together with specific boundary configurations. The physical behavior of a model simulates (in a known manner) the physical behavior of the prototype.

There are several types of similarity. Geometric similarity exists when the ratios of all homologous dimensions, between the model and the prototype, are the same. The geometric scale ratio, or length ratio, is denoted by  $L_r = L_p/L_m$ , where the subscripts  $p$  and  $m$  refer to prototype and model, respectively.

Kinematic similarity, or similarity of motion, implies that the ratios of velocities and accelerations between the model and prototype are equal.

Dynamic similarity requires that the ratios of homologous forces between the model and prototype be the same. In hydraulic problems, the primary forces that influence the flow are the forces due to gravity, viscosity, pressure, surface tension, and elasticity. The inertial force is the vector sum of all the others [5]. The following dimensionless numbers relate inertial force to each of the forces listed above.

$$\text{Froude number (inertia/gravity), } F = \frac{V}{\sqrt{Lg}} \quad (1)$$

$$\text{Reynolds number (inertia/viscosity), } R = \frac{VL}{\nu} \quad (2)$$

$$\text{Euler number (inertia/pressure) } = \frac{\rho V^2}{\Delta p} \quad (3)$$

$$\text{Weber number (inertia/surface tension) } = \frac{\rho L V^2}{\sigma} \quad (4)$$

$$\text{Cauchy number (inertia/elasticity) } = \frac{\rho V^2}{E} \quad (5)$$

It is apparent that a model fluid cannot simulate all of these properties at once. However, in most cases several of the forces will be absent or negligible in the model. Therefore, a model can usually simulate the critical forces in the prototype for a certain type of flow.

Hydraulic similitude. - The flow through a fuse plug is primarily determined by gravity and inertia forces; the other forces may be neglected. The ratios between the model and prototype are determined from the Froude law (equation 1). The scale relations according to the Froude law are listed below:

<u>Ratio</u>	<u>Scale relation (prototype/model)</u>
Length	= $L_r$ (geometric ratio)
Area	= $L_r^2$
Volume	= $L_r^3$
Time	= $t_r' = \frac{L_r^{1/2}}{g_r} = L_r^{1/2}$ (for $g_r = 1$ )
Velocity	= $V_r = L_r/t_r' = L_r^{1/2}$
Discharge	= $Q = L_r^{5/2}$

Dimensional analysis. - Vanoni [6] discusses the important variables involved in the present knowledge of sedimentation in a section on "Fundamentals of Sediment Transport." He reduced the sediment discharge rate,  $Q_s$ , to the following relationship. These symbols are defined in the list at the front of this paper.

$$Q_s = F(Q, d, \nu, \rho, \rho_s, \sigma_g, w, g) \quad (6)$$

The following sections will address each of the variables in equation 6.

Sediment transport. - Models involving erosion of noncohesive bed material must simulate tractive stress ( $\tau_0$ ), since the tractive stress causes the drag force required to overcome the forces holding a particle in place (fig. 2-5).

The tractive stress on a particle fluctuates because of the turbulence. The drag force and turbulence are a function of the Reynolds number (equation 2). Therefore, a model operated according to Froude scaling does not necessarily simulate the tractive forces and sediment erosion accurately. In some models the sediment sizes must be adjusted to compensate for a Reynolds number that is too low.

Shields developed a diagram relating dimensionless shear stress ( $\tau^*$ ) to a boundary or grain Reynolds number ( $R^*$ ). Shields used this diagram to define critical shear stress,  $\tau_c$  (the stress required for incipient motion of sediment). This concept has been expanded by others to include dimensionless unit sediment discharge.

$$(q_s^* = \frac{q_s}{u^*d})$$

Taylor [6] has shown that dimensionless unit sediment discharge at low transport levels falls very close to the Shields curve for incipient motion. Figure 2-6 shows that for  $R^*$  less than 100, the sediment discharge rate increases for a given dimensionless shear ( $\tau^*$ ). The dimensionless shear is actually a function of the Froude number and the density ratio of the sediment and the fluid.

$$\tau^* = \frac{\tau_0}{(\gamma_s - \gamma) d} = \left(\frac{u^{*2}}{gd}\right) \left(\frac{\gamma}{\gamma_s - \gamma}\right) \quad (7)$$

where:

$$R^* = u^*d/\nu$$

$$u^* = \sqrt{\tau_0/\rho} = \sqrt{gRS} = V \sqrt{f/8}$$

$$\frac{u^{*2}}{gd} = \text{Froude number}$$

and,

$$\left(\frac{\gamma}{\gamma_s - \gamma}\right) = \text{density ratio}$$

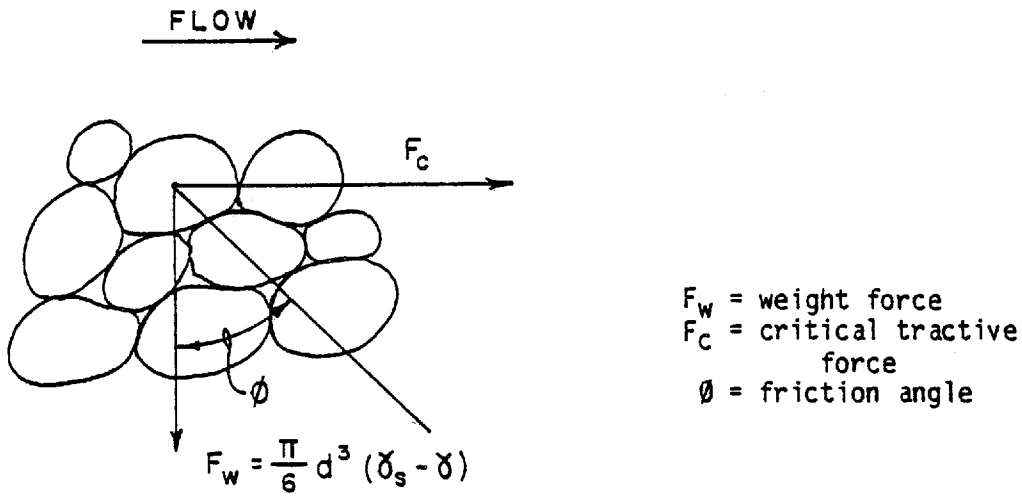


Figure 2-5. - Forces on a sediment particle.

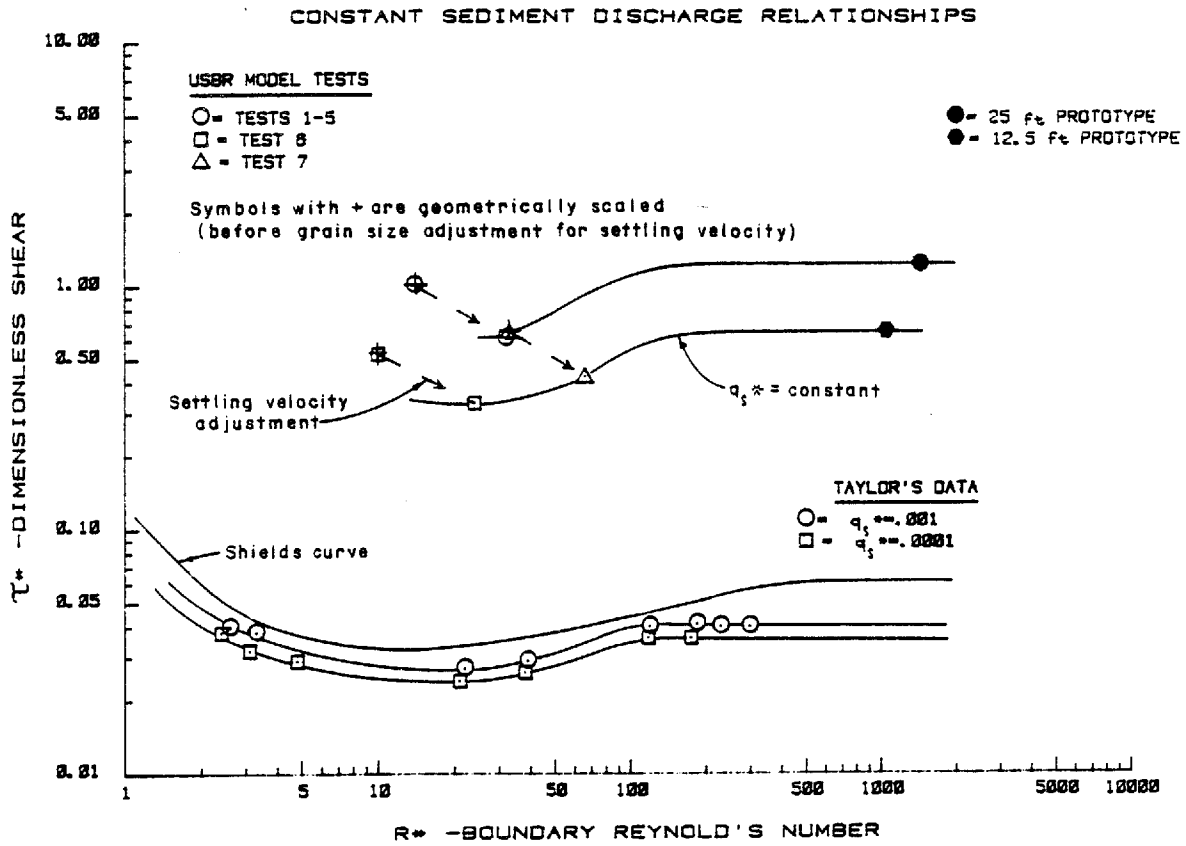


Figure 2-6. - Dimensionless unit sediment discharge versus dimensionless shear and boundary Reynolds number.

Figure 2-6 shows that a model scaled according to the Froude law ( $\tau^* = \text{constant}$ ) will erode too rapidly in the range from  $5 < R^* < 100$ . A diagram of settling velocity (fig. 2-7) also illustrates that small particles settle at a slower rate and require less tractive force to move.

For particle diameters above 1 mm, the settling velocity ( $w$ ), is a function of the particle diameter ( $d$ ) to the 1/2 power. This is consistent with Froude scaling ( $V_r = L_r^{1/2}$ ).

Settling velocity adjustment. - By increasing the size of a model sediment grain, the settling velocity can be corrected to Froude scaling. According to geometric scaling, a 1:10 scale model of prototype sand 2.0 mm in diameter would use sand 0.2 mm in diameter. However, the settling velocity would then be about 0.02 m/s (see fig. 2-7) when it should be 0.049 m/s, according to Froude scaling. If the model particle size is increased from 0.2 mm to 0.4 mm, the settling velocity is corrected to 0.049 m/s, the proper value for Froude scaling.

The effect of the settling velocity adjustment on the dimensionless sediment discharge rate ( $q_s^*$ ) is shown on figure 2-6. The symbols with a "+" are computed according to geometric scaling. Note that the model values of  $\tau^*$  are about the same as the prototype values they simulate. Tests 1-5 simulate the 25-foot prototype, and tests 6 and 7 simulate the 12.5-foot prototype. However, the model value of  $q_s^*$  must be the same in the model and prototype to properly scale the time rate of sediment transport. When the model grain sizes are adjusted for settling velocity (as described above) the value of  $\tau^*$  decreases while the value of  $R^*$  increases. This brings the model value of  $q_s^*$  much closer to the projected prototype value of  $q_s^*$  (see fig. 2-6). In this study, the model grain sizes were computed using this method of settling velocity adjustment to account for the low boundary Reynolds number. This method applies to noncohesive materials in the model and the prototype, and must be checked for each grain size and each model flow condition. If the model Reynolds number ( $R^*$ ) was even lower, the model sediment density ( $\rho_s$ ) could be adjusted to match  $q_s^*$ .

Erosion rate scale ratio. - After the settling velocity adjustment described above, the erosion rate scales according to the Froude law. Velocities scale according to  $L_r^{1/2}$ ; therefore, the erosion rate ( $E_1$ ) also scales according to  $L_r^{1/2}$ .

The model tests conducted for the Oxbow Project used prototype materials in the model. For these materials, Tinney and Hsu [1] concluded that the erosion rate ratio would be,  $(E_1)_r = L_r^{1/3}$ . Chee [4] derived the following equation for the erosion rate ratio,

$$(E_1)_r = L_r^{(0.375)} (S_s - 1)_r^2 d_r^{0.13}$$

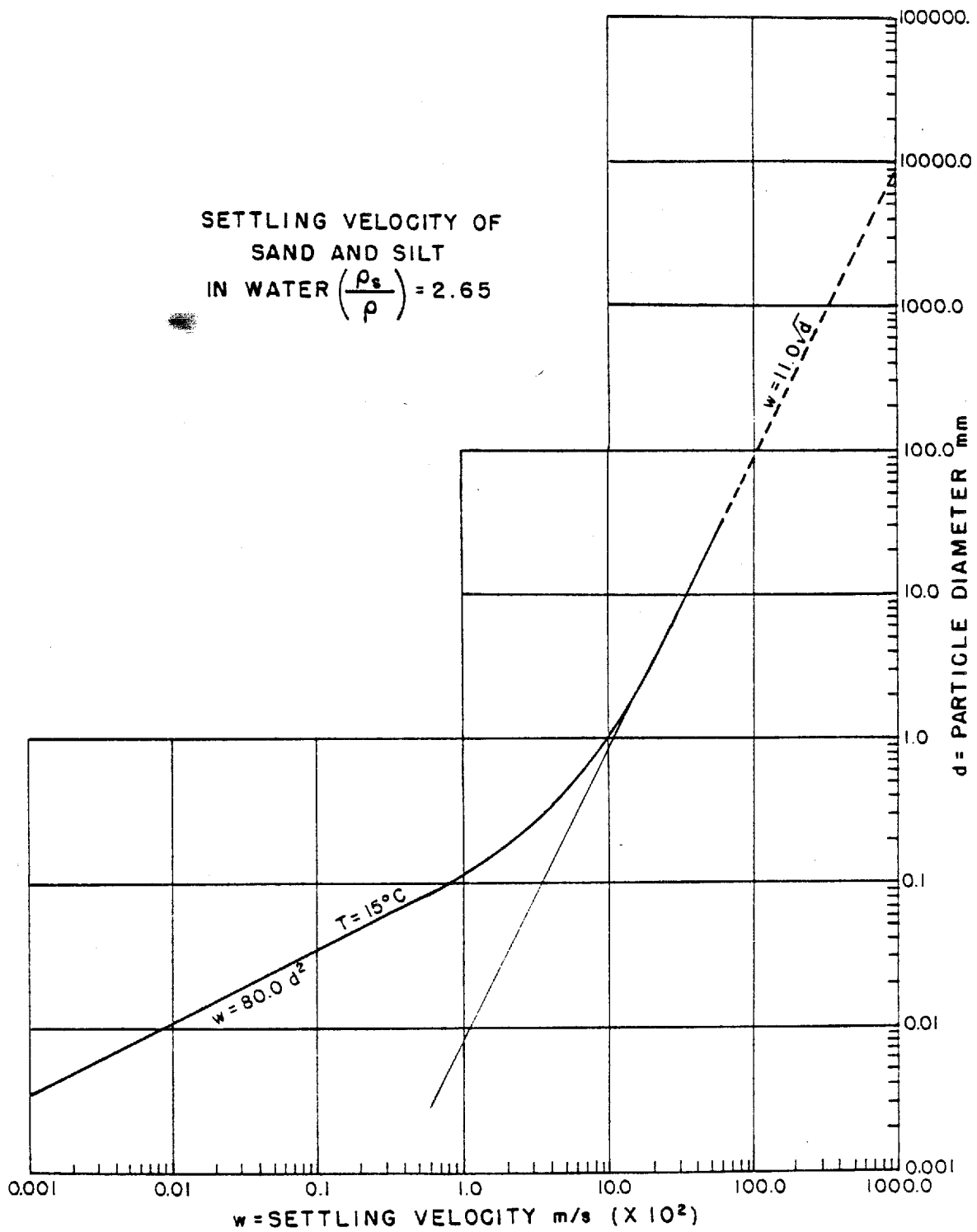


Figure 2-7. - Settling velocity of sand and silt in water  
 $(\rho_s/\rho) = 2.65$ .

where  $S_s$  is the sand specific gravity. If  $(S_s - 1)_r = 1$  and  $d_r = L_r$  (geometric scaling), then  $[E_1]_r = L_r^{0.505}$ . This is very close to the Froude scaling ratio obtained in the analysis,  $(E_1)_r = L_r^{1/2}$ . For  $(S_s - 1)_r = 1$  and  $d_r = 1$ , the erosion rate ratio derived by Chee is also close to that derived by Tinney and Hsu,  $(L_r)^{-0.375}$  versus  $(L_r)^{1/3}$ .

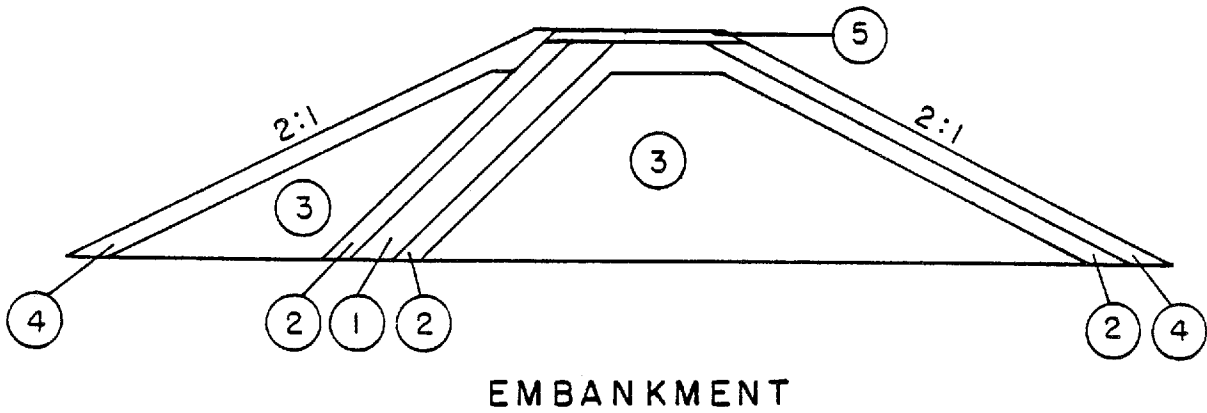
However, it is much more desirable to use model particles of a size close to the geometric scale, because prototype-sized materials in a model do not simulate the correct number of particles per unit volume or the contact force between the grains. In addition, the drag force on the model particles is not correct when the model particles are prototype size.

Embankment design. - The model fuse plug embankment was designed with the same zones found in most zoned earth or rockfill dams. The arrangement of these zones is shown on figure 2-8. The main difference between a fuse plug embankment and a typical rockfill or earthfill dam is the arrangement of the impervious core. The core is inclined so that when the downstream material is washed away, pieces of the core break off because of bending under its own weight and the water load. The core material is normally silt or clay. The sand filter will prevent piping through cracks that may develop in the core. The filter will also keep windblown silt and clay from infiltrating the downstream embankment material. The compacted sand and gravel and compacted rockfill are designed to be noncohesive and easily erodible once the washout process begins. The prototype gradation curves for each zone are shown on figure 2-9. A range of acceptable sizes are shown with the gradation simulated in the model study indicated by a dashed line.

The model and prototype gradation curves for each zone are shown on figures 2-10 through 2-13. These model gradation curves were determined by making settling velocity adjustments to the grain sizes determined by geometric scaling.

The pilot channel section was designed to wash out quickly once the water has started to flow through the pilot channel. A slightly larger rockfill material with fewer sand sizes was used in this section to ensure a rapid break. The prototype pilot channel was designed to be 0.9 m (3 ft) deep, allowing for a 0.3 m (1 ft) water depth and 0.6 m (2 ft) of freeboard. This depth of water was determined to be adequate to initiate a breach during the Oxbow study. The width of the pilot channel was investigated in this model study. The side slopes of the pilot channel were set at 1:1; however, this value could be varied in the prototype. The gradation and compaction of the noncohesive materials are very important factors in determining the erosion rate. As the materials are compacted, more tractive force is required to remove the grains since there are more grains per unit volume and more contact and interlocking between the grains. A well-graded mixture of grains will require more tractive force to erode than uniform-sized material. The smaller particles will fill the voids between the larger particles, making the mixture heavier per unit volume and creating more contact between the particles.

- ① CORE MATERIAL
- ② SAND FILTER
- ③ COMPACTED SAND AND GRAVEL
- ④ SLOPE PROTECTION
- ⑤ GRAVEL SURFACING



- ⑥ COMPACTED ROCKFILL

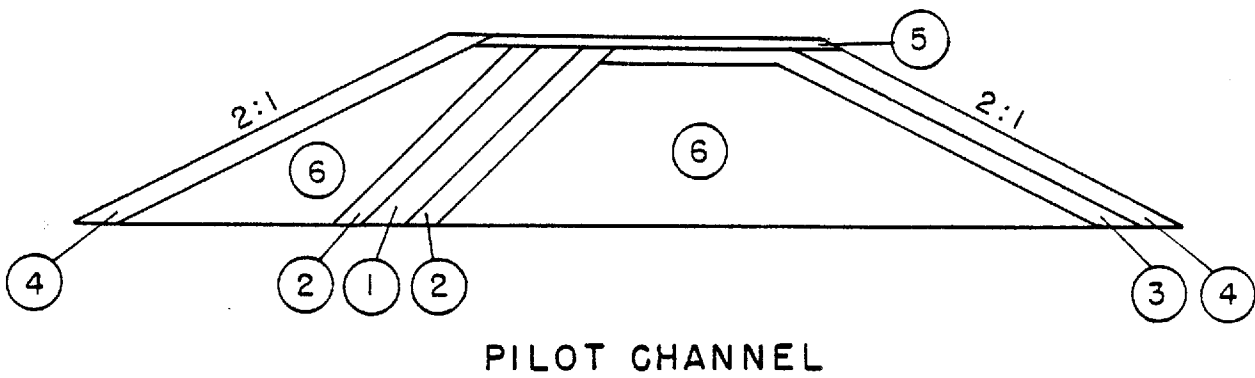


Figure 2-8. - Fuse plug embankment and pilot channel.

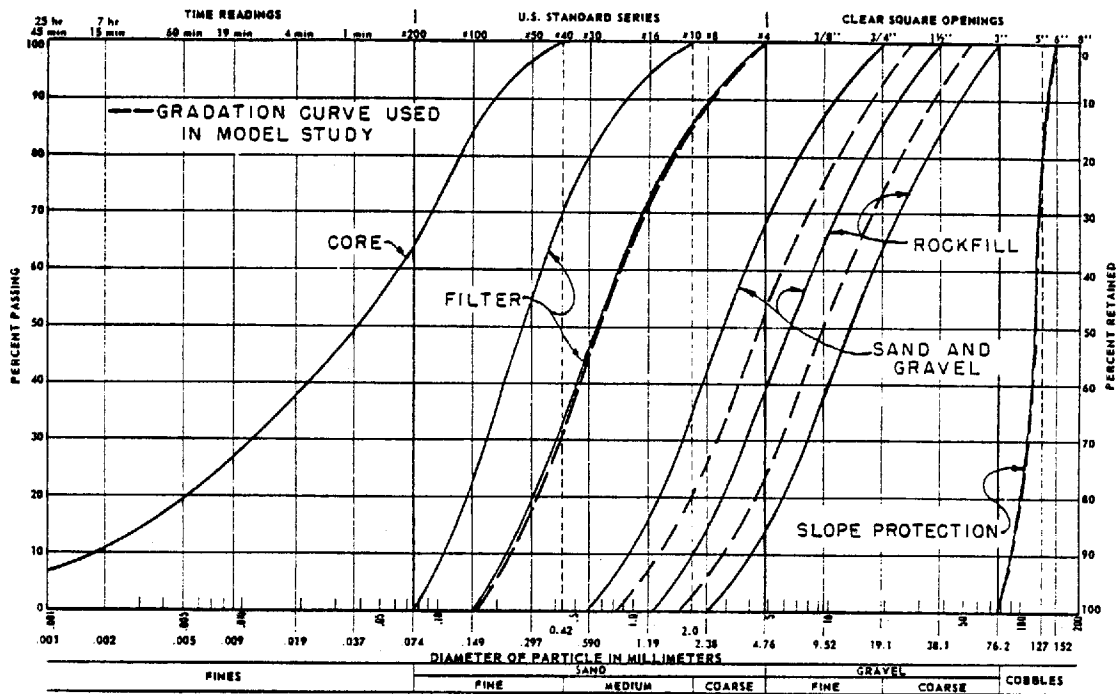


Figure 2-9. - Prototype gradation curves.

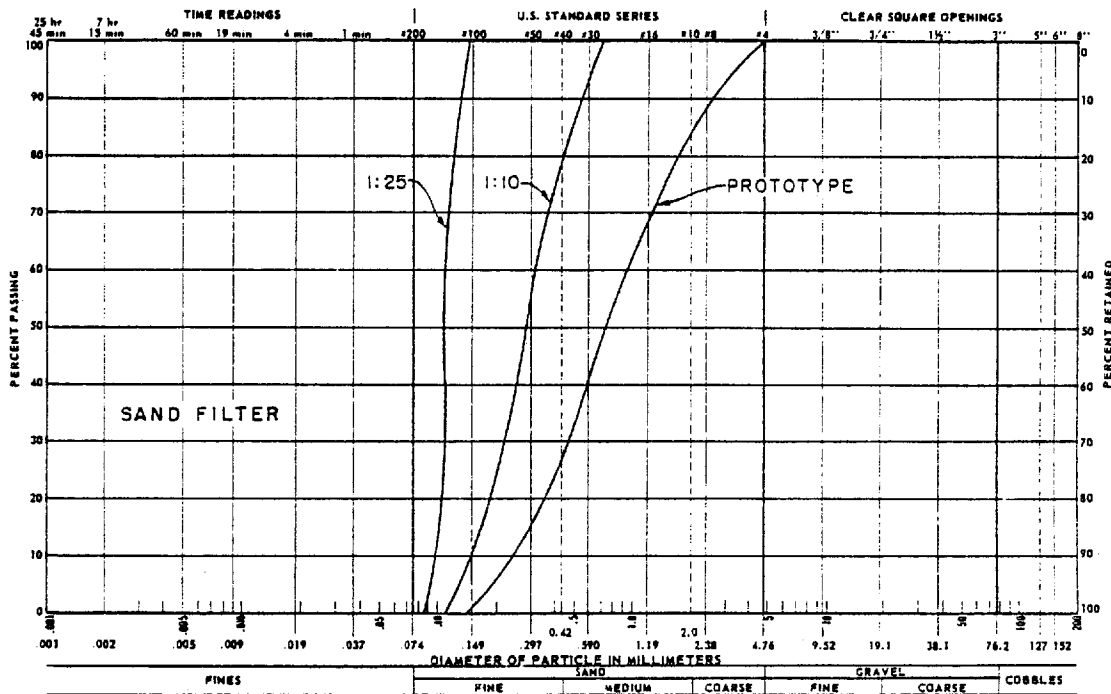


Figure 2-10. - Gradation curves, sand filter.

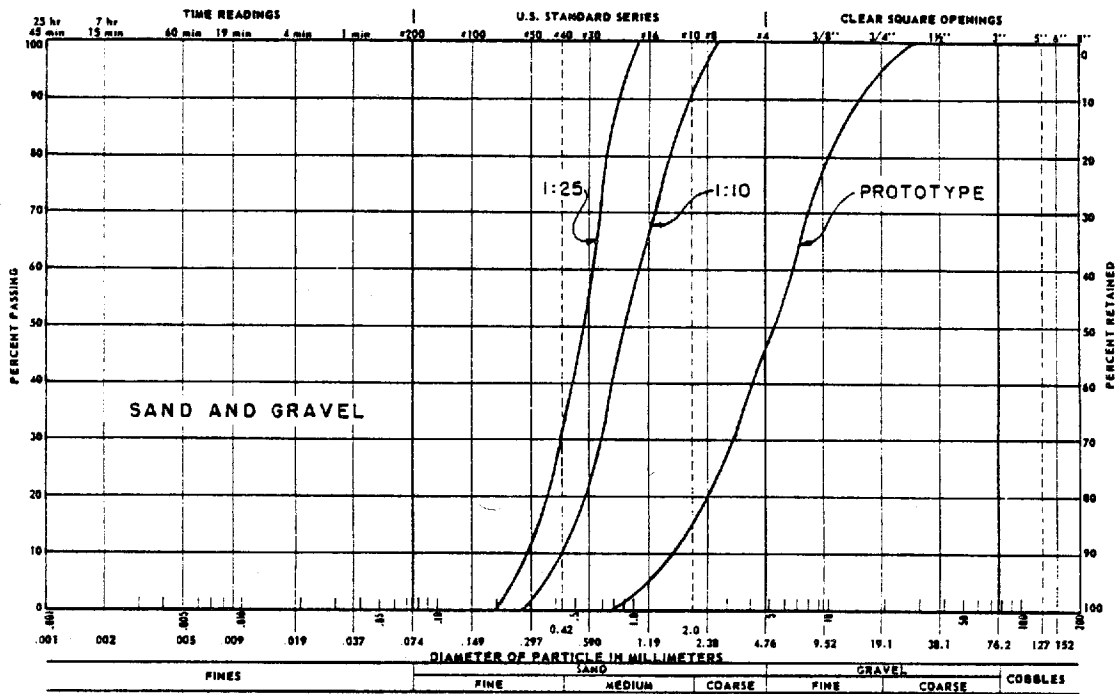


Figure 2-11. - Gradation curves, sand and gravel.

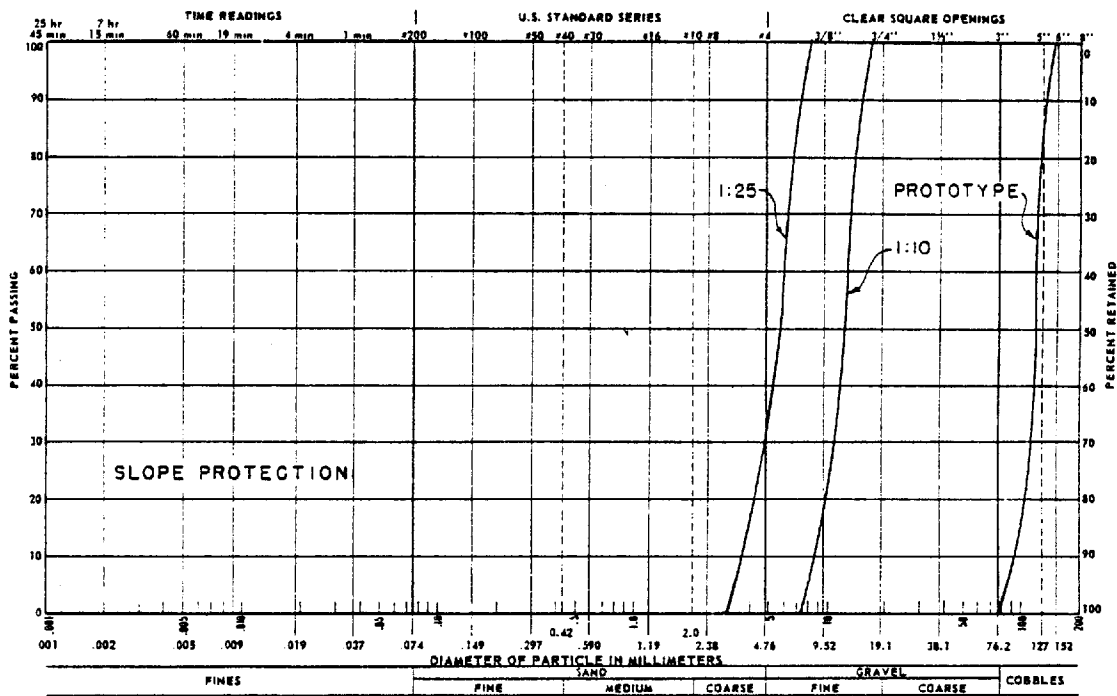


Figure 2-12. - Gradation curves, slope protection.

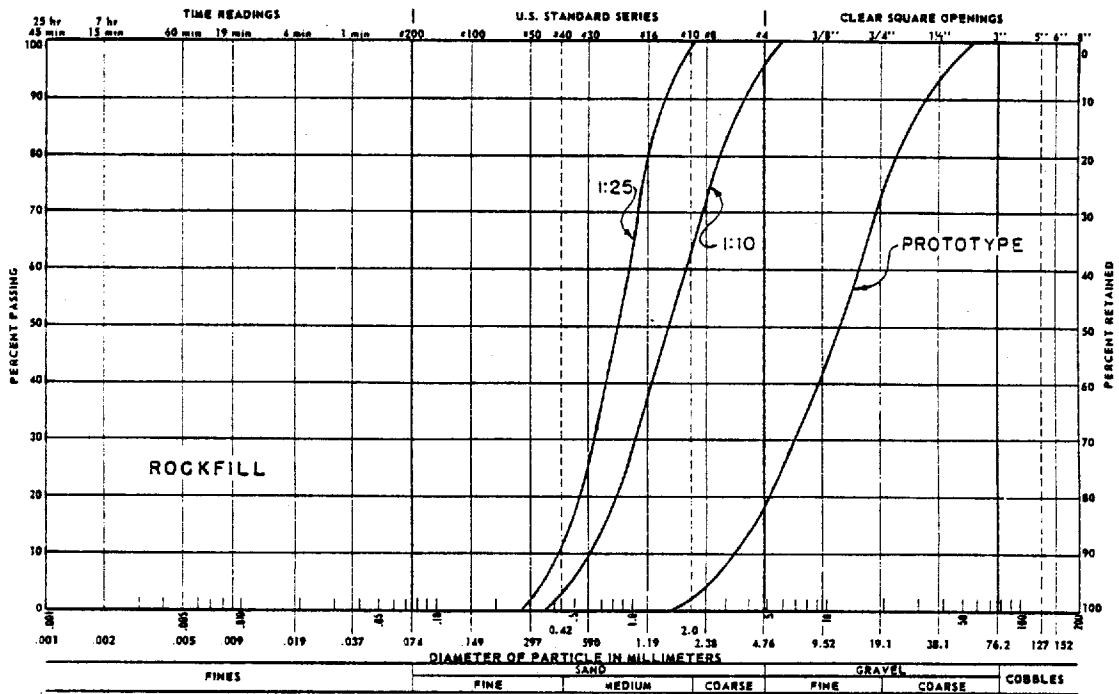


Figure 2-13. - Gradation curves, rockfill.

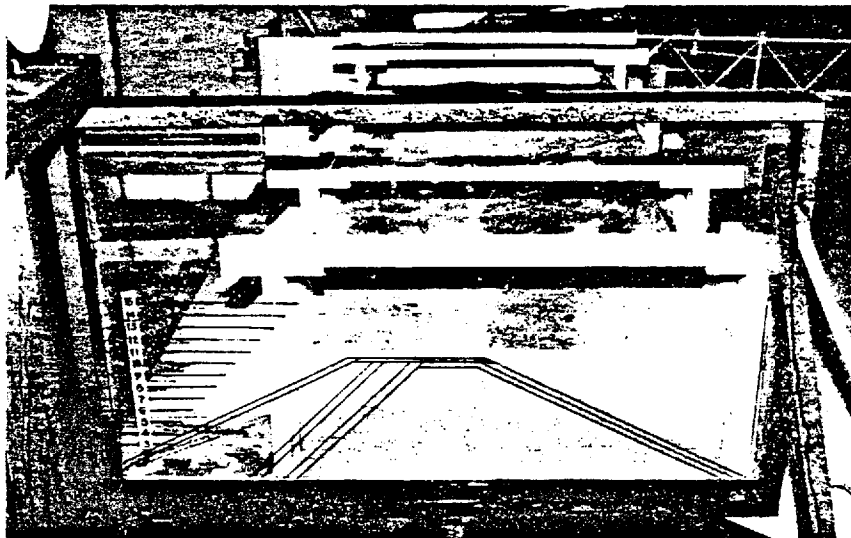


Figure 2-14. - Model placement.

For these reasons, great care was taken in placing the model fuse plug embankments. Relative density tests were conducted on the model materials (see gradation curves on figs. 2-10, 2-11, and 2-13.) The materials were then placed in the model at 70 percent relative density.

The method used consisted of placing a predetermined weight of material in a given volume to obtain 70 percent relative density. The proper proportion of each of the material sizes was mixed to obtain the desired gradation. A known weight of the mixture was then placed in a known volume in the model (fig. 2-14). The volume in the model was controlled by using wooden forms 38 to 51 mm (1-1/2 to 2 in) thick. The main embankment downstream from the core (zones 3 and 6 on fig. 2-8) was placed in layers using this method. The compaction was obtained by using a compressed-air powered vibrator and tamping tools. When the placement of this zone was complete the forms were removed and the corners trimmed to the correct slope. The sand filter, core, embankment upstream from the core, slope protection, and gravel surfacing were then weighed and applied using templates and tamping tools. A completed model fuse plug embankment is shown on figure 2-15.

The model fuse plug embankments were all placed in the same manner to ensure consistency between tests. Since the materials were similar to the prototype in gradation ( $\sigma_g$ ) and relative density, the erosion rates determined in the model should correctly simulate prototype erosion rates.

Structural similitude. - The impervious core was not simulated as part of the hydraulic modeling because the cohesive clay portion does not fail as a result of sediment erosion. The core is designed to break off in pieces from the weight of the water and embankment material above it, as the non-cohesive material downstream washes away. Figure 2-16 is a schematic diagram illustrating the failure mode of the materials in the pilot channel. The core fails in a similar manner during the lateral erosion process, as the material on the face of the embankment downstream from the core is washed away.

The structural behavior of the core material was simulated qualitatively, because the prototype core material strength will vary a great deal. A structural analysis of the prototype core as a cantilevered slab indicates that only about 0.88 m (2.9 feet) of core would overhang horizontally before it would break (assuming a high tensile strength in the core of 6895 KPa (1000 lb/in<sup>2</sup>)).

The structural behavior of the core material is governed by gravity and elasticity forces. The structural merit number (M) is the dimensionless ratio of gravity forces to elasticity forces.

$$M = \left( \frac{\gamma L}{E} \right) \quad (8)$$

where E = Modulus of elasticity of the core.

For structural similitude,

$$\left(\frac{\gamma L}{E}\right)_m = \left(\frac{\gamma L}{E}\right)_p \quad (9)$$

If  $\gamma_m = \gamma_p$  then

$$\frac{E_p}{E_m} = \frac{L_p}{L_m} = L_r \quad (10)$$

The ratio of the moduli of elasticity must equal the model scale ratio. However, it is difficult to find a model core material that has a modulus of elasticity low enough to satisfy this ratio and also maintain a seal. Therefore, a mixture of 10 percent clay and 90 percent sand with a modulus of elasticity approximately equal to that of the prototype was used. The thickness of the clay core portion of the model was reduced instead of using a material with a lower modulus of elasticity.

Because the model modulus of elasticity ( $E_m$ ) was too large, the core thickness needed to be reduced to compensate. A clay core reduced in thickness (1/3 of geometric scaling) was used in most of the tests. This thickness resulted from computing the correct moment of inertia in the model to compensate for the modulus of elasticity being too large in the model. The remainder of the core thickness was built with sand sprayed with a stabilizing agent.

#### Model Measurements

During each test several measurements were made to document the washout.

1. Discharge was recorded at 3-second intervals. The measurement weir flow was subtracted from the total (initial) flow to obtain the flow through the breach.
2. The reservoir level was recorded continuously.
3. Flags were placed at 1 foot intervals on the top of the embankment, and a grid pattern was painted on the downstream face of the embankment. The lateral erosion rates ( $E_l$ ) were recorded by noting the time that the erosion reached each flag. These rates were checked by viewing the videotape.
4. Each test was filmed using videotape cameras, still photographs, and slides. One video camera was located downstream from the embankment, and the other filmed the washout through the acrylic plastic end wall.
5. The discharge, reservoir level, and time were recorded on magnetic disk with the aid of a microcomputer.

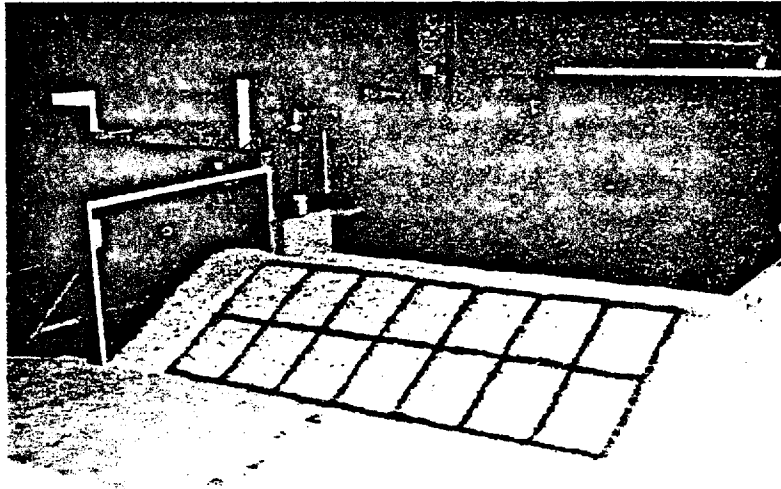


Figure 2-15. - Fuse plug embankment after placement.

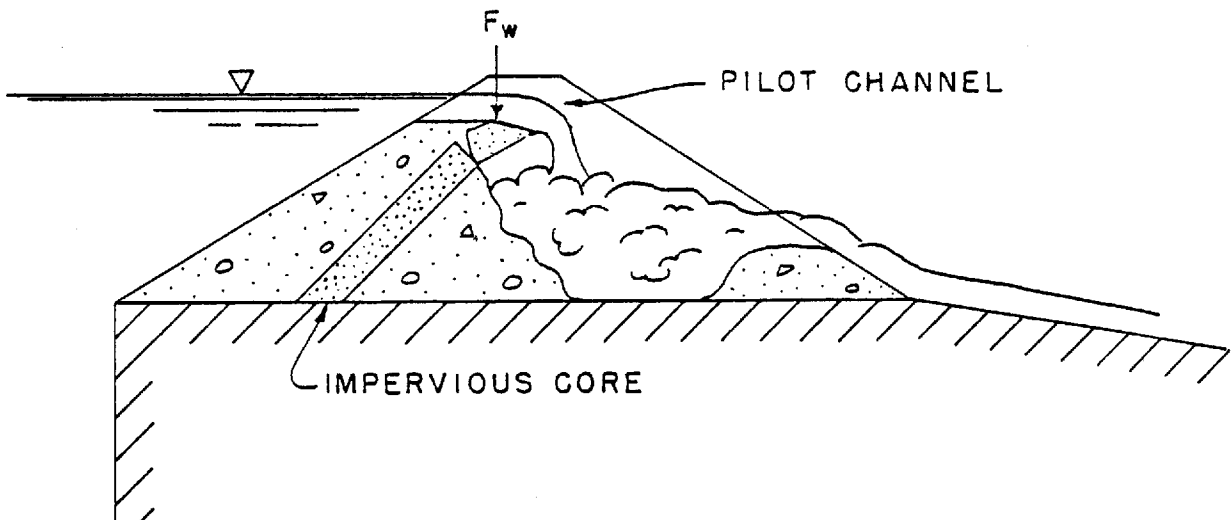


Figure 2-16. - Flow through the pilot channel showing the failure mode of the impervious core.

## Model Results

The erosion process and lateral erosion rate are dependent on the geometric configuration of the embankment. Figure 2-17 shows the configuration of the model embankments and defines the symbols. Table 2-1 lists the values of each of the pertinent features for each test. These values are listed as a dimensionless ratio of the fuse plug height (H).

The rate of erosion was consistent for any one model configuration and flow condition (see figs. 2-18 through 2-25). The erosion rate varied as the model configuration or flow condition was changed. The first number in the regression equations, shown on each graph, is the lateral erosion rate in ft/min.

Before each test the reservoir level was held constant at a level below the pilot channel elevation, with a long adjustable weir. The test was begun by raising the water surface to a level equivalent to a 0.3 m (1 ft) water depth in the prototype pilot channel. The material downstream of the core eroded down to the base of the fuse plug. When the support was removed from beneath, a piece of the core broke off. This process then reoccurred until the material in the pilot channel was completely washed away. Figure 2-26 is a series of photographs illustrating the erosion process.

After the initial breach, the embankment eroded laterally. The flow eroded the face of the embankment downstream from the core in a steady, continuous manner. As the noncohesive material washed away removing support, pieces of the core broke off. Figure 2-27 is a schematic diagram illustrating how water flowed around the core and eroded the downstream embankment.

## ANALYSIS

An analysis was made of the model results to determine the effect of the pertinent geometric and flow parameters.

### Effect of Embankment Design Features

Core. - The role and effect of the impervious core was analyzed in the model study. A previous section on "Structural Similitude" discusses the structural modeling of the core. A clay core 1/3 of the thickness indicated by geometric scaling was used during most tests.

To assess the effect of the core thickness on the lateral erosion process, one test was conducted with a clay core thickness indicated by geometric similitude (test No. 2). This thickness was about 3 times more than that required for structural similitude. During this test the initial breach proceeded about the same as the other tests until the first core break, when the core overhung and did not break. The first break was assisted by manually breaking the clay, after which the washout process proceeded much the same as in the other tests. The lateral erosion rate was 0.463 m/min (1.52 ft/min). This erosion rate was only 2 percent less

Table 2-1. - Fuse plug model test data

Test No.	Date 1983	H (ft)	w/H	B/H	b/H	$\theta$ (deg)	T/H	t/H	L/H	p/H	h/H	Sand filter	D/J	D/H	$E_1$ (ft/min)
1	2-14	1.0	0.4	4.4	3.1	45	0.12	0.04	0.0	0.24	0.12	Yes	0.21	0.92	1.74
2	2-28	1.0	0.4	4.4	3.1	45	0.12	0.12	0.12	0.36	0.12	No	0.21	0.92	1.52
3	3-10	1.0	0.4	4.4	4.0	30	0.12	0.04	0.32	0.48	0.12	No	0.21	0.92	1.53
4	3-21	1.0	0.4	4.4	3.1	45	0.12	0.04	3.24	0.48	0.12	No	0.21	0.92	1.55
5	4-4	1.0	0.8	4.8	3.4	45	0.12	0.04	0.45	0.74	0.12	Yes	0.15	0.92	1.60
6	4-11	0.5	0.8	4.8	3.4	45	0.12	0.04	0.91	1.48	0.24	Yes	0.07	0.84	0.68
7	4-19	1.25	0.8	4.8	3.4	45	0.12	0.04	0.51	0.88	0.24	Yes	0.17	0.84	1.66
8	6-7	1.25	0.8	4.8	3.4	45	0.12	0.04	1.60	3.20	0.24	Yes	0.12	0.60	0.63

1 ft = 0.3048 m

\* The upstream water level (D) was lowered during test No. 7.

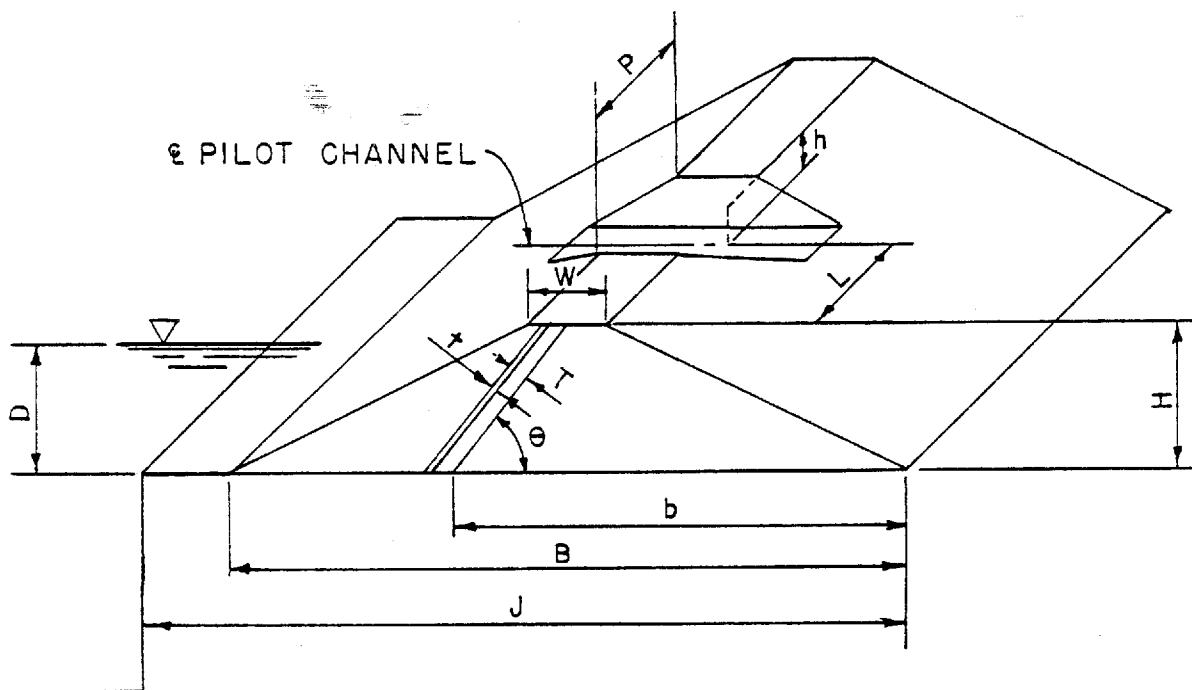


Figure 2-17. - Definition sketch of geometric features of model fuse plug embankment.

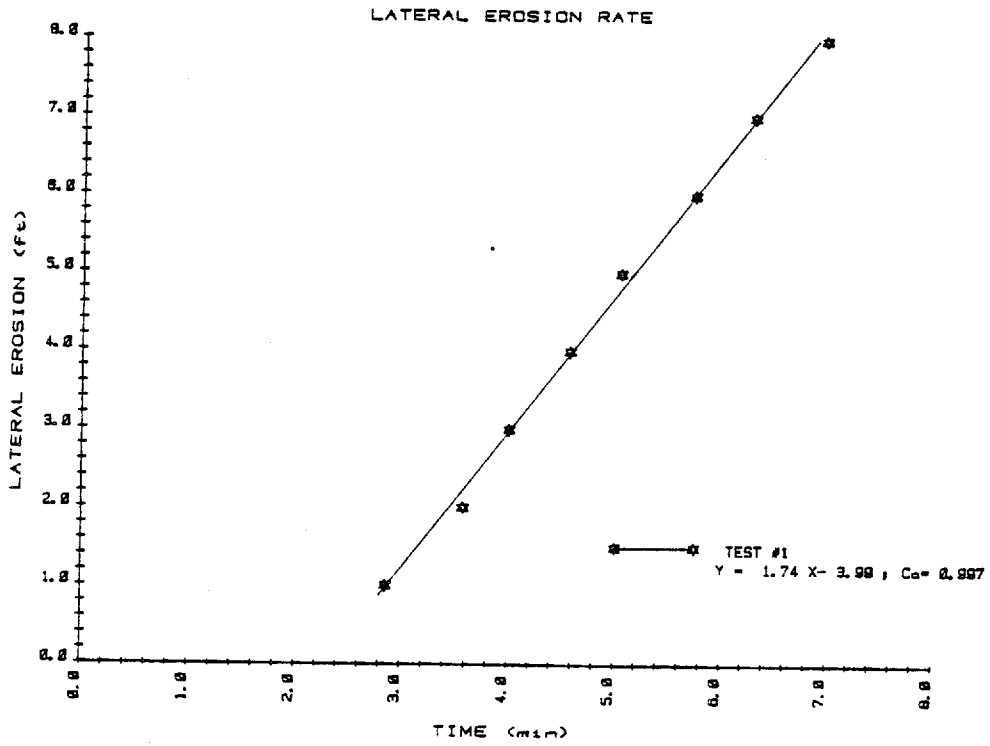


Figure 2-18. - Lateral erosion rate, test No. 1

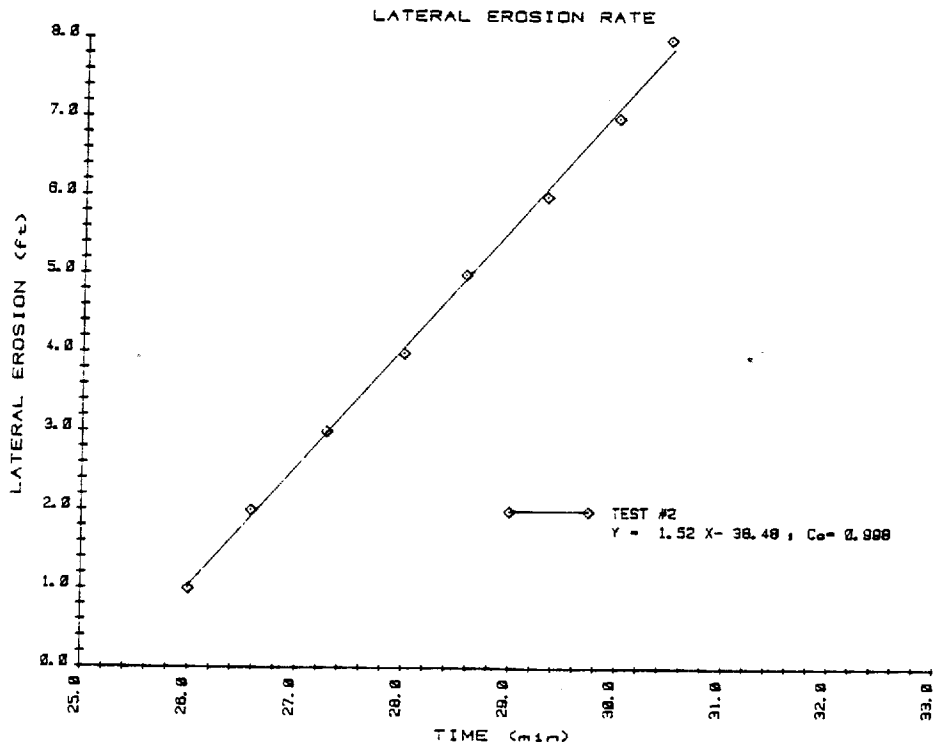


Figure 2-19. - Lateral erosion rate, test No. 2.

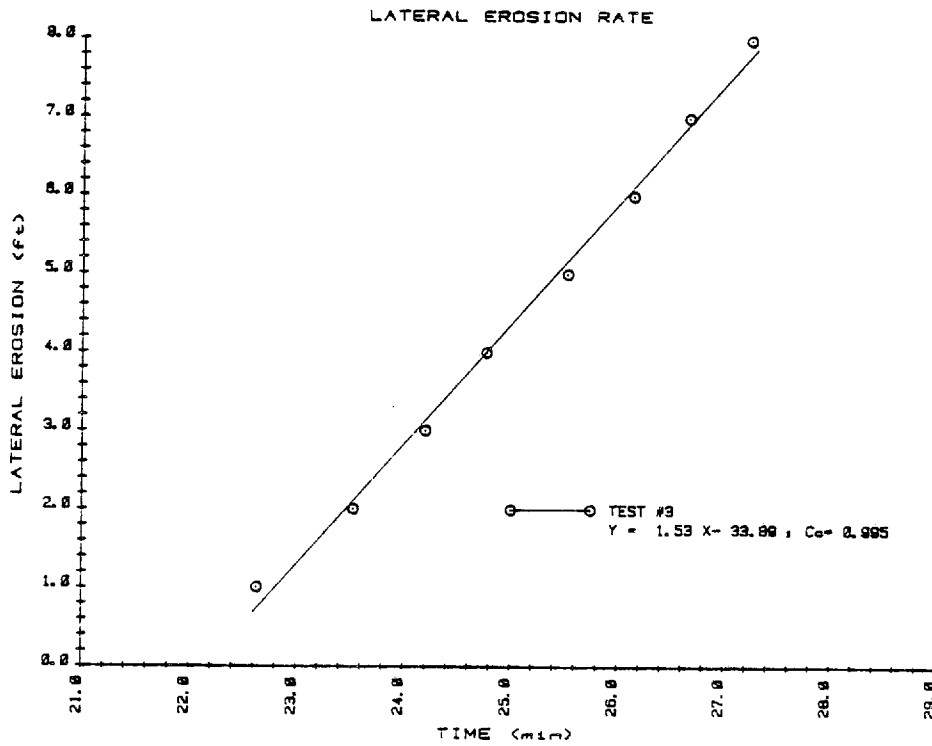


Figure 2-20. - Lateral erosion rate, test No. 3.

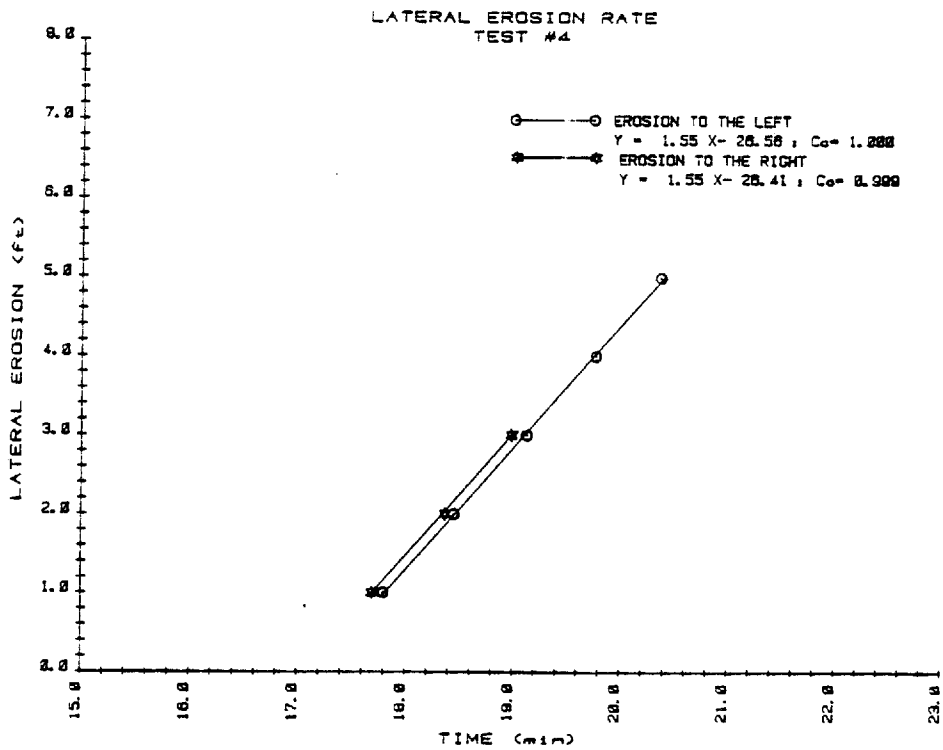


Figure 2-21. - Lateral erosion rate, test No. 4.

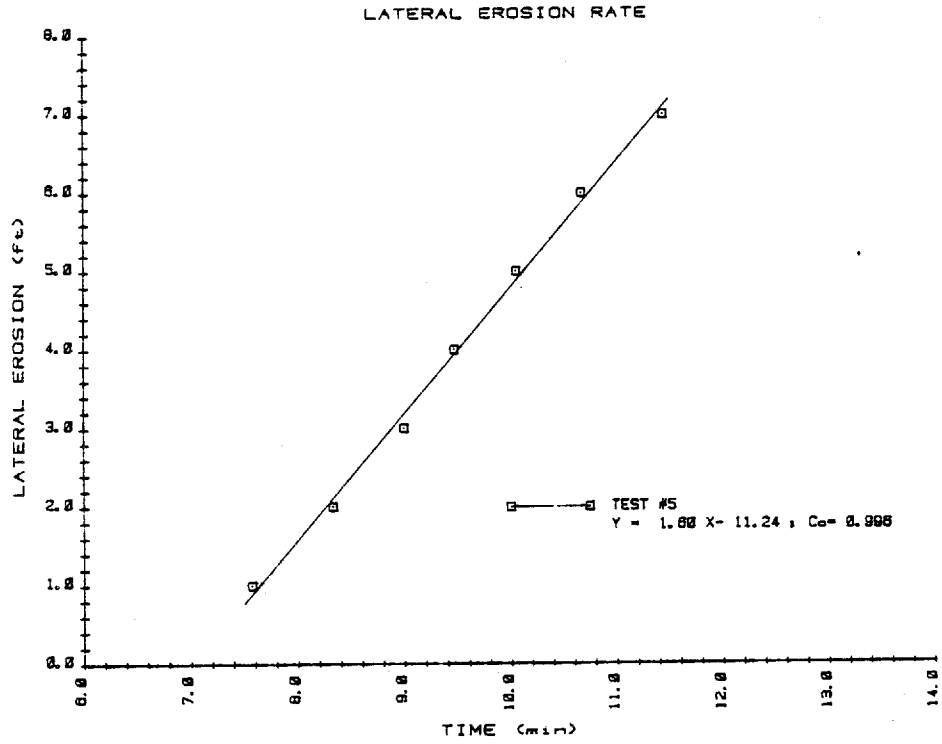


Figure 2-22. - Lateral erosion rate, test No. 5.

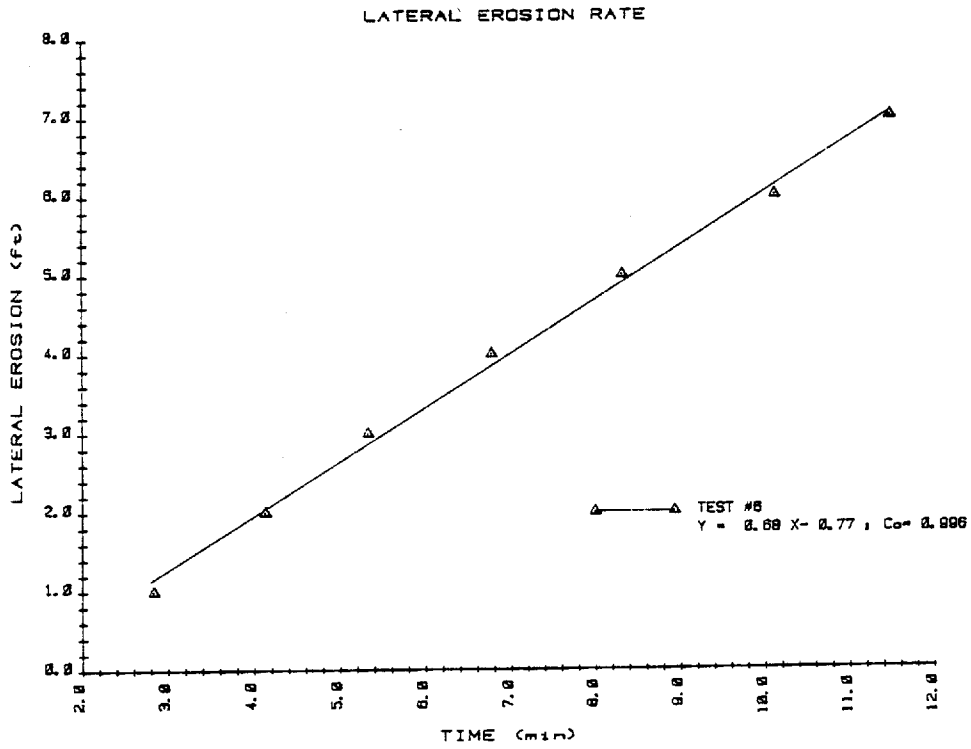


Figure 2-23. - Lateral erosion rate, test No. 6.

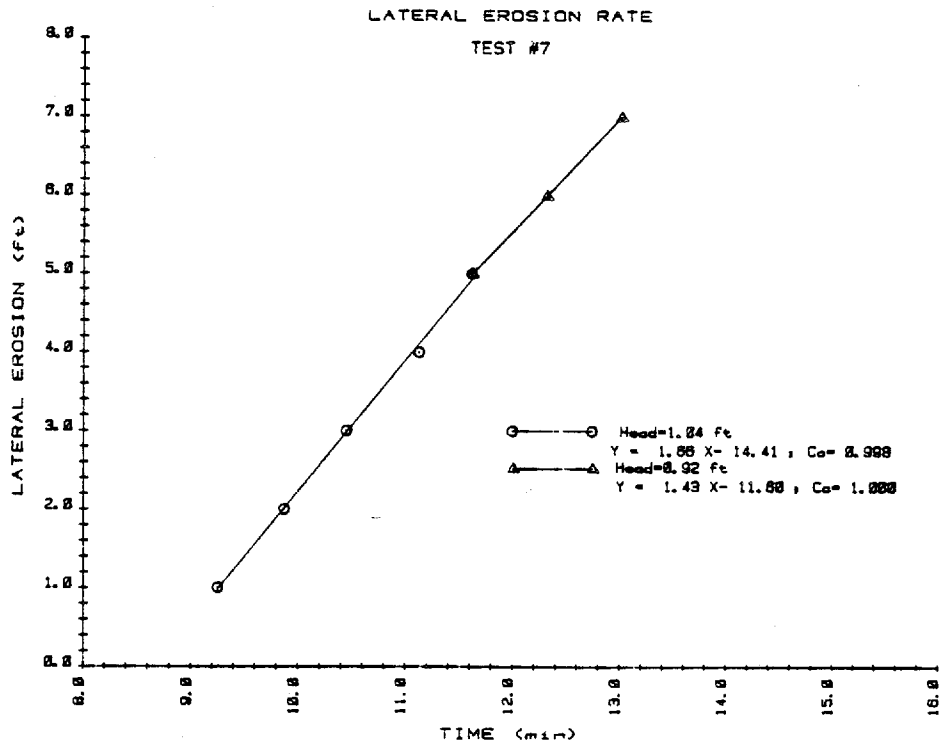


Figure 2-24. - Lateral erosion rate, test No. 7.

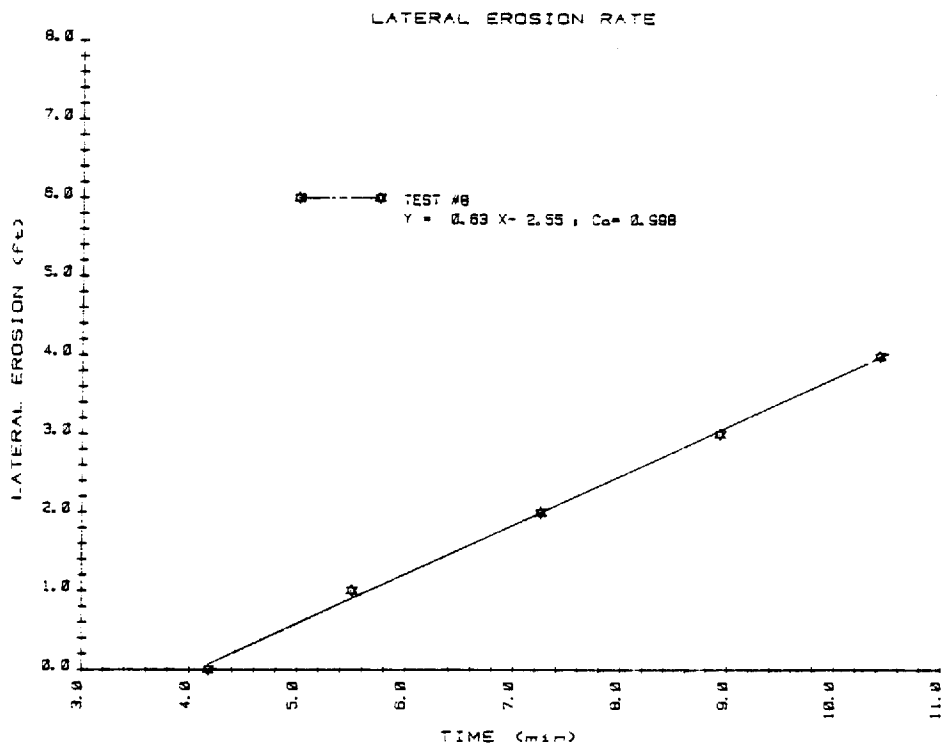
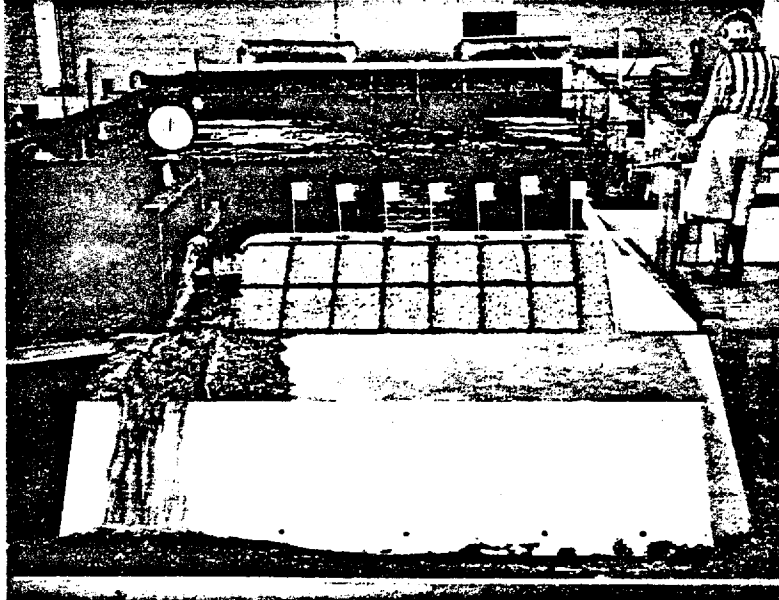
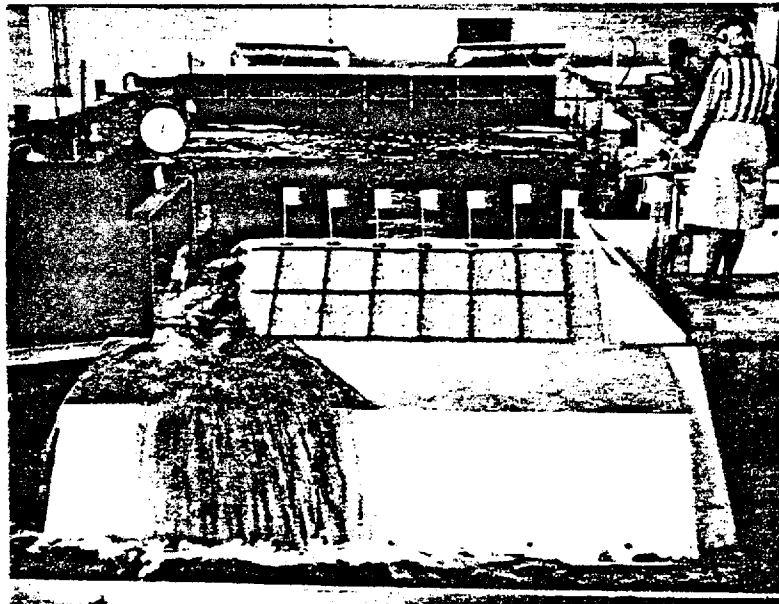


Figure 2-25. - Lateral erosion rate, test No. 8.

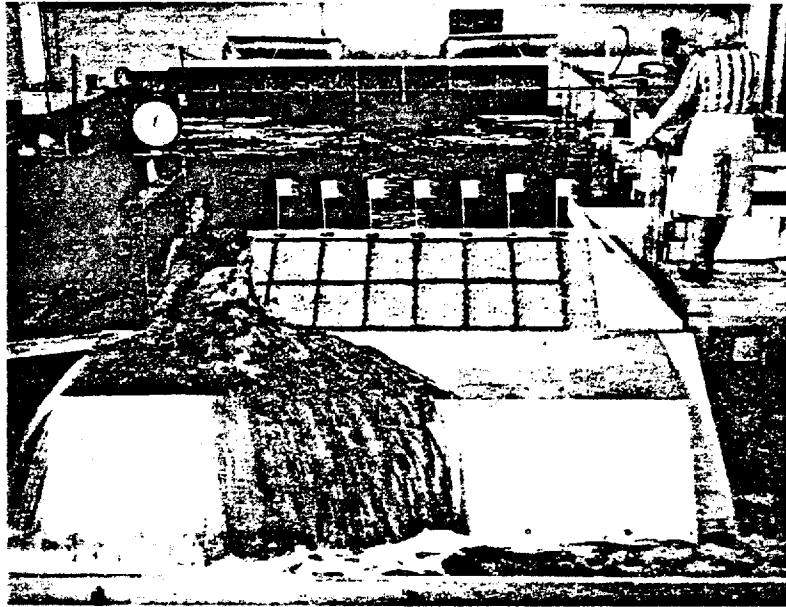


(a) Water flowing through the pilot channel over the clay core.

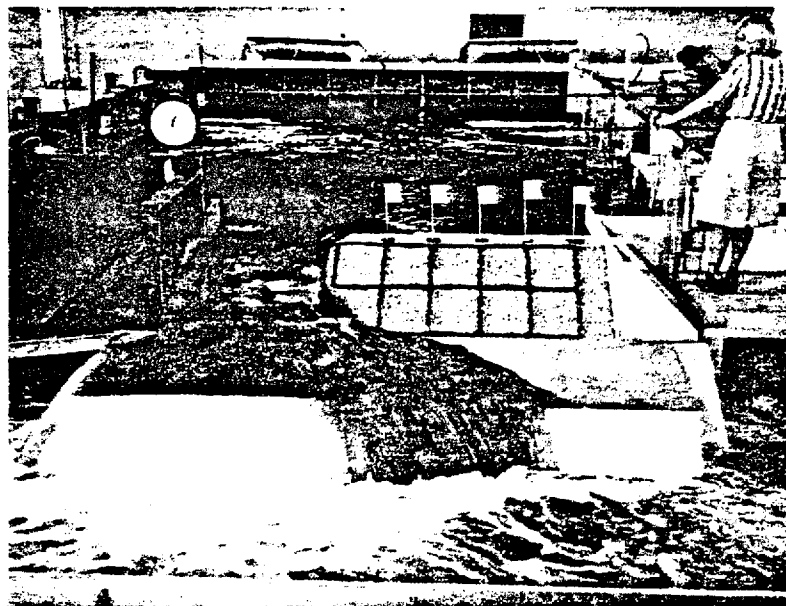


(b) After initial breach

Figure 2-26. - Photographs illustrating the washout process (sheet 1 of 3).



(c) The lateral erosion process is underway.



(d) The lateral erosion rate was determined by timing the erosion between flags.

Figure 2-26. - Photographs illustrating the washout process (sheet 2 of 3).



(e) The reservoir elevation was held constant by the long adjustable weir in the background.



(f) The erosion process is almost complete.

Figure 2-26. - Photographs illustrating the washout process (sheet 3 of 3).

than that in an identical test with a thinner clay core (test No. 4,  $E_1 = 0.472$  m/min (1.55 ft/min)). During the lateral erosion process in test No. 2, the noncohesive material downstream from the core eroded at a constant rate and the core broke off in bigger pieces than in the other tests.

This test indicates that the lateral erosion rate is a function of the erosion rate of the noncohesive material and not a function of the core strength.

During test No. 3 the core was installed at an angle  $30^\circ$  above horizontal. The material downstream from the core was shielded by the core and the initial breach took longer. The lateral erosion rate was about the same. It was decided to use a core angle of  $45^\circ$  during future tests to prevent shielding of the downstream materials.

Pilot channel. - Various widths and positions of the pilot channel were tested. The location of the pilot channel did not have a noticeable effect on the lateral erosion rate. The erosion rate for test No. 4, with the pilot channel located near the center of the embankment, was the same in both directions, and about the same as a similar test with the pilot channel close to the end of the embankment.

The width of the pilot channel controls the amount of water passing through to initiate the breach. The model tests indicate that the pilot channel width ( $p$ ) should be at least  $1/2$  of the fuse plug height ( $p/H \geq 0.5$ ).

Sand filter. - Tests were run with and without the sand filter surrounding the main embankment downstream from the core. (See fig. 2-8 for embankment zoning.) It was found that the sand filter has a significant effect on both the initial breach and the lateral erosion. Without the filter the water flowing through the pilot channel infiltrates the downstream noncohesive material and partially saturates this zone, thus prolonging the breaching process. With the more permeable filter the water flowing through the pilot channel infiltrates down the face of the core. The pilot channel erosion process proceeds much more rapidly. The lateral erosion rate is significantly slower when the downstream sand filter is removed. Test No. 1 and test No. 4 have identical embankment designs, with the exception of the sand filter. The erosion rate without the sand filter is about 11 percent slower. The volume of the compacted sand and gravel zone is greater without the sand filter, since it also occupies the sand filter zone. The compacted sand and gravel requires more tractive force to move because these particles are larger and their sizes vary more than those in the sand filter material.

Size of embankment. - The relative size of the embankment was investigated in test No. 5. The width of the fuse plug crest was doubled, thereby increasing the area of the eroding face of the embankment. The erosion rate for Test No. 5 was about 8 percent less than for test No. 1. This is about the same percentage as the increase in the area of the downstream compacted sand and gravel zone.

### Hydraulics of Flow Through the Opening

Broad-crested weir. - Flow through the opening is the same as flow over a broad-crested weir. Broad-crested weir flow is dependent on the depth of water above the crest (D) and the length of the crest (J). In the range  $0.08 < D/J < 0.5$  [7], flow over a horizontal crest will be in the broad-crested weir flow range. Figure 2-28 shows broad-crested weir flow profiles for test Nos. 6, 7, and 8. For broad-crested weir flow the top surface and flow streamlines become parallel with the horizontal crest. The flow discharge is controlled by the critical flow depth near the end of the crest [8].

Discharge coefficients. - The following equation expresses discharge over a weir as a function of water depth.

$$Q = CLH^{3/2} \quad (11)$$

For critical depth,  $d_c = (2/3)H$ , and using the Froude number at critical depth:

$$F = 1 = \frac{V}{\sqrt{gd_c}} \quad (12)$$

Equation 12 can be expressed as

$$\begin{aligned} \text{or} \quad q &= g^{1/2} (2/3)^{3/2} H^{3/2} \\ q &= 3.09 H^{3/2} \end{aligned}$$

where the unit discharge,  $q = Vd_c$

The coefficient (C) in equation 11 is 3.09.

For a broad-crested weir, the critical depth point is actually slightly upstream from the downstream end of the crest, and losses reduce the theoretical value of C slightly. Empirical data [7] indicate that in the broad-crested weir range  $0.08 \leq D/J \leq 0.5$  the theoretical discharge coefficient is reduced by a factor of 0.848. Therefore, equation 11 would be:

$$\begin{aligned} \text{or} \quad Q &= (0.848)(3.09)LH^{3/2} \\ Q &= (2.62)LH^{3/2} \end{aligned} \quad (13)$$

Discharge coefficients measured during test No. 7 are shown on figure 2-29. These coefficients were computed from the discharge and water depth measurements made during the test. The discharge coefficients increase to a maximum value of 2.78 for a breach length (L) of 1.2 to 1.8 m (4 to 6 ft). The coefficient drops slightly, to  $C = 2.62$ , when the embankment is completely washed away. This value matches the empirical value for a broad-crested weir.

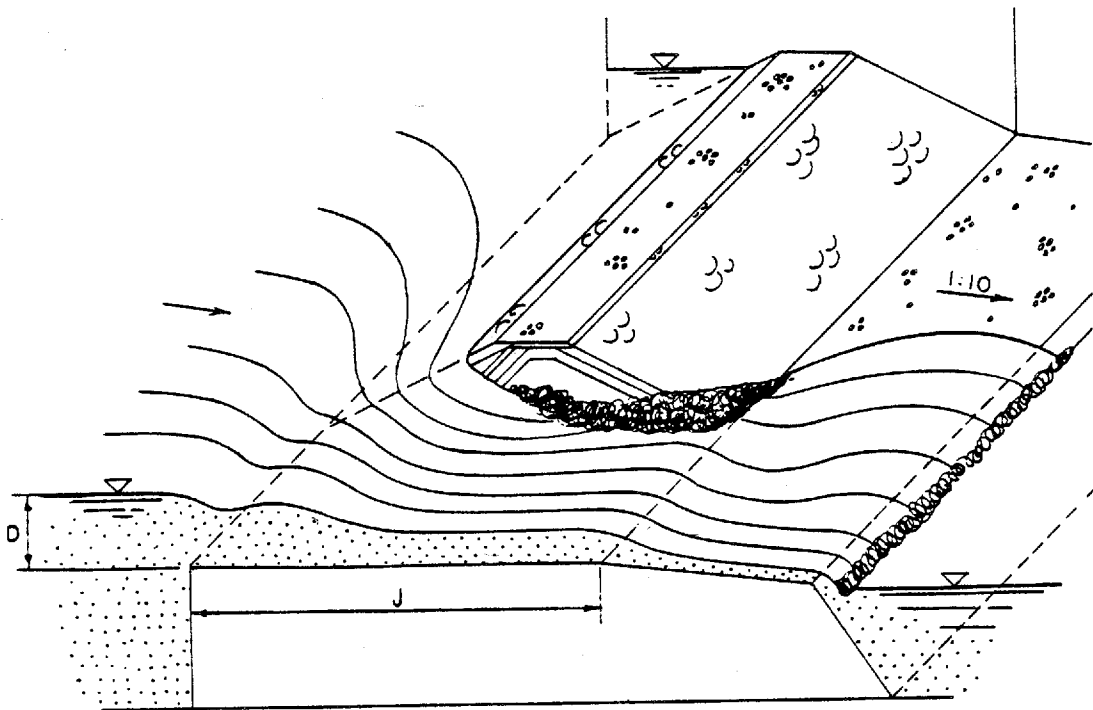


Figure 2-27. - Schematic of lateral erosion process. The water flows across the face of the embankment, around the core, and erodes the noncohesive material downstream from the core.

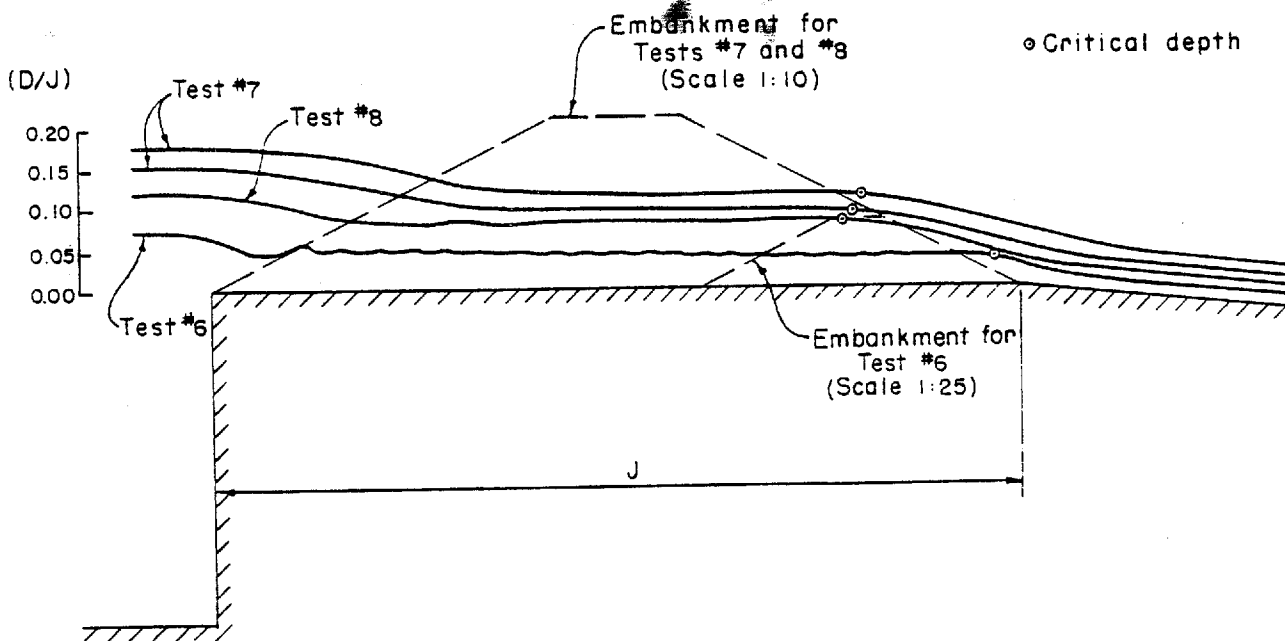


Figure 2-28. - Broad-crested weir flow profiles, test Nos. 6, 7, and 8.

(equation 13). The higher discharge coefficient during the washout can be attributed to a longer effective weir length caused by the flow coming around the face of the embankment (fig. 2-27). During test No. 6, with a relatively longer crest length, J (see fig. 2-28), the discharge coefficient during the washout was as high as 3.1.

These discharge coefficients can be used in a computer flood-routing program. The lateral erosion rate is a function of the depth to crest length ratio (D/J) and the depth to fuse plug height ratio (D/H). Tests Nos. 6 and 7 have the same D/H ratio (0.84), but different D/J ratios (see fig. 2-28). The result is a different erosion process. For (D/J) > 0.12, the flow surface was still drawing down as it reached the embankment. This caused a longitudinal vortex along the face of the downstream compacted sand and gravel that accelerated the erosion rate. For D/J < 0.12 the flow was parallel to the crest as it reached the embankment. The erosion was similar to streambank erosion with no vortex to aid the erosion process.

The lateral erosion rates are shown as a function of water depth and crest length on figure 2-30. This figure illustrates that the erosion rate is a function of the water depth squared for D/J < 0.12. For D/J > 0.12, the erosion rate is accelerated.

This analysis illustrates that the length of crest (J) has a major effect on the erosion process. It also illustrates that when it is desirable to slow the fuse plug erosion process, the length of the approach channel could be increased.

#### Projection to Prototype

The results from this study can be used to predict the behavior of a prototype fuse plug embankment. The discharge coefficients discussed in the previous sections can be used to predict flow through a given opening size.

The lateral erosion rate for a given embankment design and flow depth can be predicted from the model tests. Figure 2-31 shows the erosion rates for an embankment with dimensions given in table 2-1 for test No. 1. The flow depth was determined by the pilot channel design, with 0.6 m (2 ft) of freeboard and 0.3 m (1 ft) of water depth, regardless of the embankment height. Equation 14 can be used to estimate erosion rates for embankments of this configuration that are from 3 to 9 m (10 to 30 ft) in height.

$$E_1 = 14.6 H + 158 \quad (14)$$

where  $E_1$  is in ft/hour, and H is in feet.

If the configuration of the embankment or the flow condition is changed, the erosion rate given by equation 14 would be changed accordingly. For example, if the area of the downstream compacted sand and gravel section is increased by 10 percent, the erosion rate predicted by equation 14 should be reduced by 10 percent. If the water depth or crest length (J) are different from those on figure 2-31, the erosion rate would be adjusted using figure 2-30.

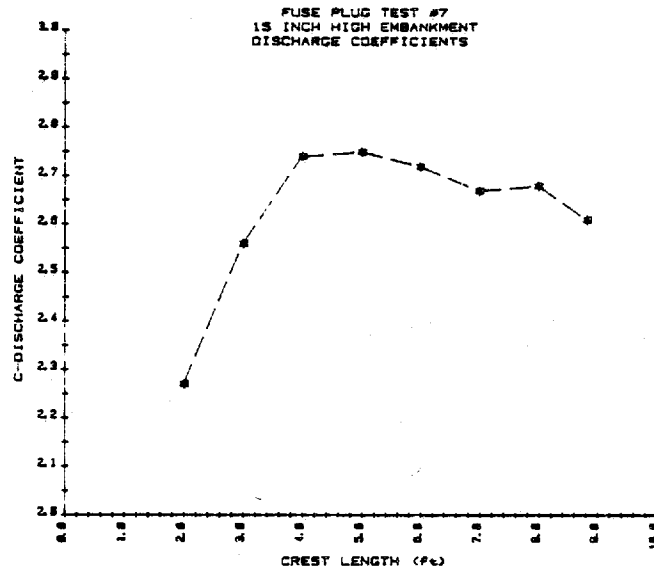


Figure 2-29. - Weir formula discharge coefficients, test No. 7.

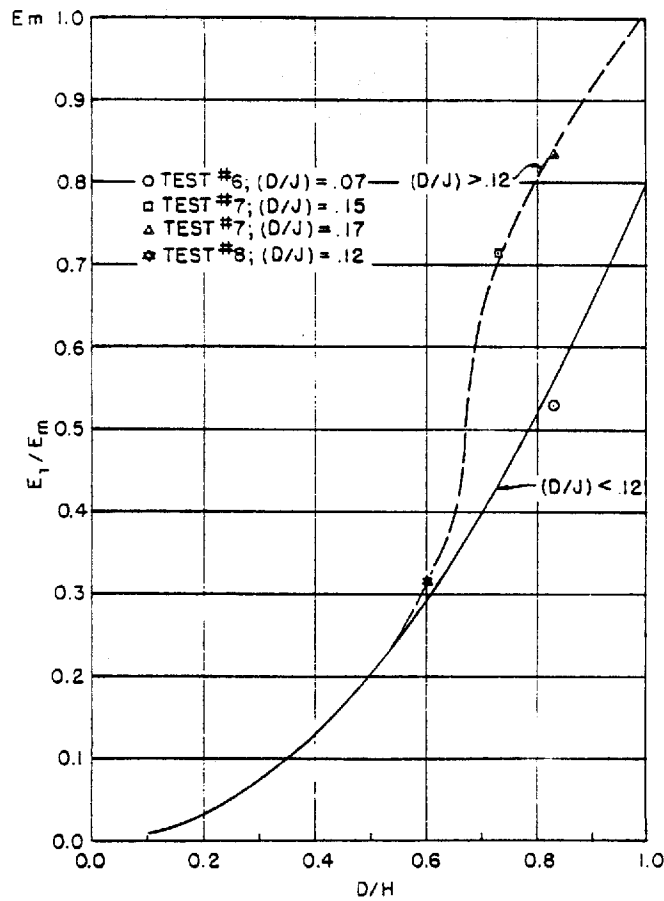


Figure 2-30. - Lateral erosion rate as a function of water depth and crest length.

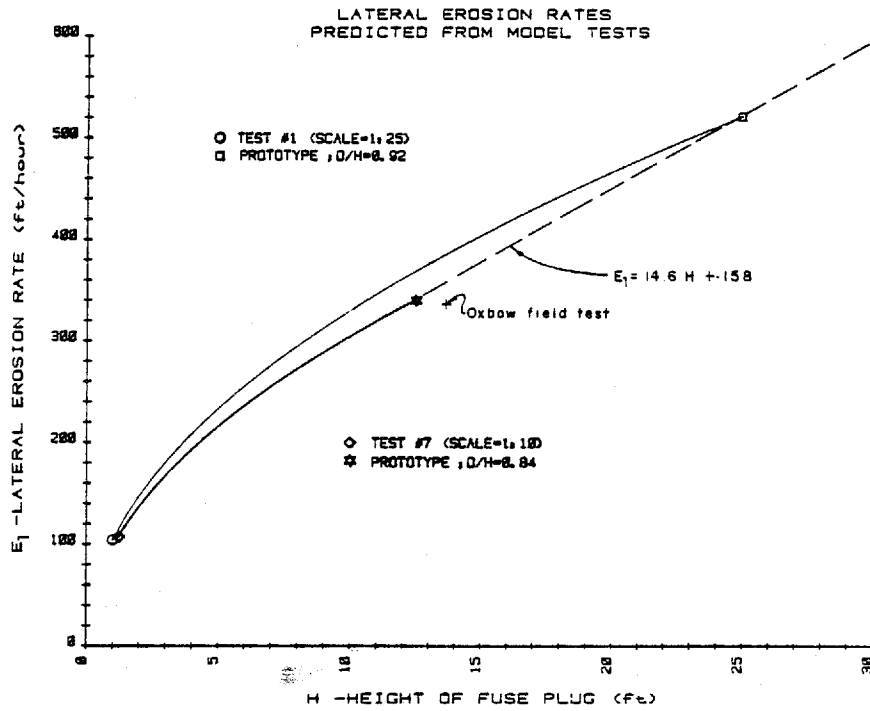


Figure 2-31. - Lateral erosion rates predicted from model tests.

- ① CORE
- ② FILTER MATERIAL
- ③ WELL GRADED MATERIAL
- ④ CONCRETE AGGREGATE

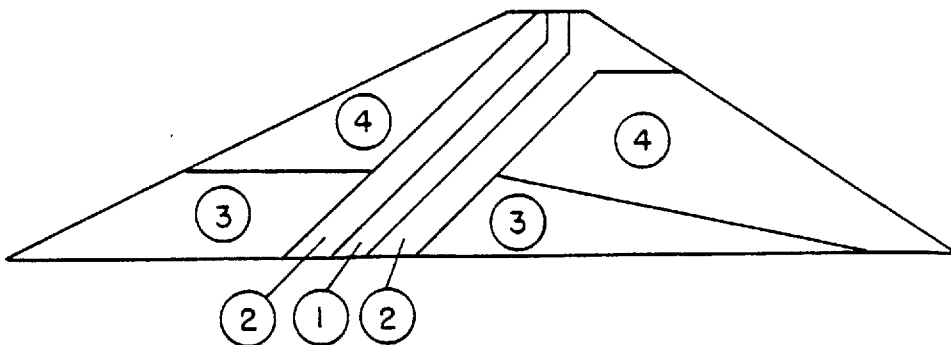


Figure 2-32. - Embankment design for Oxbow field test.

### Comparison to Oxbow Field Test

The only data available on a prototype-sized fuse plug in operation are for a field test performed as part of the design of a fuse plug control for an auxiliary spillway on the Oxbow Project on the Snake River in Idaho. The 1/2 scale field test of an 8.2 m (27 ft) prototype embankment showed the same pilot channel breach and lateral erosion process indicated by this model study. The following are the geometric and flow parameters for the Oxbow field test (as defined on fig. 2-17).

Table 2-2. - Oxbow field test data

<u>H</u> <u>(ft)</u>	<u>W/H</u>	<u>B/H</u>	<u>b/H</u>	<u>θ</u>	<u>T/H</u>	<u>L/H</u>	<u>p/H</u>	<u>h/H</u>	<u>S.F.</u>	<u>D/H</u>	<u>E<sub>1</sub></u> <u>(ft/min)</u>
13.5	0.37	4.12	2.59	45°	0.11	0.37	0.81	0.15	Yes	0.93	5.6

The Oxbow embankment design [1] is shown on figure 2-32. The gradation curve for the Oxbow zone 4 (concrete aggregate) was similar to that of zone 3 (compacted sand and gravel) in this study (fig. 2-11).

Although the embankment design for the Oxbow field test was slightly different from the embankments tested in this model study, the erosion rate was close to the erosion rate predicted by equation 14 (fig. 2-31).

During the later part of the Oxbow field test the entire embankment downstream from the sand filter was zone 3 (well graded) material. The erosion rate reduced from 102 to 22 m/hr (336 to 72 ft/hr) demonstrating the importance of material gradation.

## BIBLIOGRAPHY

- [1] Tinney, E. R., H. Y. Hsu, "Mechanics of Washout of an Erodible Fuse Plug," Journal of the Hydraulic Division, Proceedings, American Society of Civil Engineers, vol. 87, No. HY 3, May 1961.
- [2] "Oxbow Hydroelectric Development, Idaho Spillway With Fuse Plug Control, Model Studies of Fuse Plug Washout," R. L. Albrook Hydraulic Laboratory and International Engineering Company, Inc., Washington State College, Pullman, Wash., August 1959.
- [3] Hsu, H. Y., "Design of Fuse Plug Spillway," Indian Journal of Power and River Valley Development, Hydraulic Structures Special Number, vol. 91-2, pp. 308-311, 335, 1962.
- [4] Chee, S. P., "Mobile Controls for Water Resources Projects," American Water Resources, Water Bulletin, paper No. 77072, February 1978.
- [5] Morris, H. M., "Applied Hydraulics in Engineering," the Ronald Press Company, New York, N. Y., 1963.
- [6] Vanoni, Vito A., "Sedimentation Engineering," American Society of Civil Engineers, ASCE Task Committee for Preparation of the Manual on Sedimentation of the Sedimentation Committee of the Hydraulics Division, No. 54, New York, N. Y., 1975.
- [7] Bos, M. G., "Discharge Measurement Structures," Publication No. 20, International Institute for Land Reclamation Improvement, Wageningen, The Netherlands.
- [8] King, H. W., "Handbook of Hydraulics," McGraw Hill, 1963.

